# 5.5-5.8 GHz Directional Antenna with 90 Degree Phase Difference Output

**THESIS**

**ELECTRICAL ENGINEERING**
**COMMUNICATION AND INFORMATION SYSTEMS**

**Declared qualified to obtain**
**a *Master Teknik* degree**

**Irfan Mujahidin (穆逸凡)**
Student ID: 166060300111019

**UNIVERSITY of BRAWIJAYA**
**FACULTY of ENGINEERING**
**MALANG**
**2018**

# Acknowledgement

First of all, praise is to Allah SWT the almighty and the all-merciful, who has given me the guidance to complete this thesis, entitled "**5.5-5.8 GHz Directional Antenna with 90 Degree Phase Difference Output**".

My first earnest gratitude goes to to my beloved family, and the advisors, Prof. Tzyy-Sheng Horng (洪子聖), Dr. Sholeh Hadi Pramono, and Dr. Muhammad Aziz Muslim, for their bottomless kindness and sincere guidance during lab work and thesis writing.

The deepest gratitude is expressed to National Sun-Yat Sen University, University of Brawijaya, lab mate microwave laboratory of NSYSU and my friends who are eager to encourage me untill finish this master degree in electrical engineering.

Kaohsiung, July 18th 2018

Irfan Mujahidin

# Abstract

**Irfan Mujahidin,** Electric Department, Telecommunication Field, Faculty of Engineering of University of Brawijaya, Malang, 2018. Double Degree Program together with National Sun Yat-Sen University (國 立中山大學). 5.5-5.8 GHz Directional Antenna with 90 Degree Phase Difference Output. Advisor: Dr. Sholeh Hadi Pramono, Dr. Muhammad Aziz Muslim, and Prof. Tzyy-Sheng Horng / 洪子聖

The wireless sensor network system requires two antennas that have an output 90 phase difference as a comparison and use a very expensive material for high frequency. 5.5 – 5.8 GHz microstrip antenna frequency equipped with two output 90 degree phase difference in one antenna has been proposed. This thesis presents a 5.5 – 5.8 GHz microstrip antenna with 90-degree phase difference outputs. The presented antenna consists of a circular patch, a reflector, a pair of feedlines with via holes and a branch-line coupler. The measurement results indicate that the antenna outputs have a phase difference of 86.38 º at 5.5 GHz and 90.98 º at 5.8 GHz. Moreover, the measured gain of the antenna is 3.67 dBi at 5.5 GHz and 5.45 dBi at 5.8 GHz. The overall size of the antenna is 70 mm × 35 mm on an FR4 substrate with dielectric constant of 4.4

***Keywords :*** Microstrip antenna, branch-line coupler, 90-degree phase difference.

# RINGKASAN

**Angger Baskoro**, Departemen Elektro, Bidang Telekomunikasi, Fakultas Teknik Universitas Brawijaya, Malang, 2018. Program *Double Degree* bekerja sama dengan *National Sun Yat-Sen University* (國立中山大學). 5.5-5.8 GHz Directional Antenna with 90 Degree Phase Difference Output. Pembimbing: Dr. Sholeh Hadi Pramono, Dr. Muhammad Aziz Muslim, and Prof. Tzyy-Sheng Horng / 洪子聖

Sistem jaringan sensor nirkabel membutuhkan dua antena yang memiliki keluaran perbedaan fasa 90 derajat sebagai pembanding dan menggunakan material yang sangat mahal untuk frekuensi tinggi. antena mikrostrip dengan frekuensi 5.5 - 5.8 GHz dilengkapi dengan dua keluaran perbedaan fase 90-derajat dalam satu antena telah diusulkan. Tesis ini menyajikan antena mikrostrip yang memiliki frkuensi 5.5 - 5.8 GHz dengan keluaran beda fase 90 derajat. Antena yang disajikan terdiri dari patch melingkar, reflektor, sepasang feedlines dengan melalui lubang dan penggandeng branch-line. Hasil pengukuran menunjukkan bahwa output antena memiliki perbedaan fase 86,38 º pada 5,5 GHz dan 90,98 º pada 5,8 GHz. Selain itu, gain yang diukur dari antena adalah 3,67 dBi pada 5,5 GHz dan 5,45 dBi pada 5,8 GHz. Ukuran keseluruhan antena adalah 70 mm x 35 mm pada substrat FR4 dengan konstanta dielektrik 4.4

**Kata kunci:** Antena mikrostrip, penggandeng bercabang, perbedaan fasa 90 derajat.

# 摘要

无线传感器网络系统需要具有输出 90 相位差的**两个**天线作为比较，并且使用非常昂贵的材料用于高频。 已经提出了在**一个**天线中配备有**两个**输出 90 度相位差的 5.8GHz 微带天线频率。 本文介绍了一种具有 90 度相位差输出的 5.5 - 5.8 GHz 微带天线。 所呈现的天线包括圆形贴片，反射器，具有通孔的一对馈线和分支线耦合器。 测量结果表明，天线输出在 5.5 GHz 时的相位差为 86.38º，在 5.8 GHz 时的相位差为 90.98º。 此外，天线的测量增益在 5.5 GHz 时为 3.67 dBi，在 5.8 GHz 时为 5.45 dBi。 在 FR4 基板上，天线的整体尺寸为 70 mm×35 mm

，介电常**数**为 4.4

**關鍵字:** 微带天线，分支线耦合器，90 度相位差。

# Table of Contents

# List of Tables

# List of Figure

# Chapter 1 INTRODUCTION

## 1.1 Background

The antenna plays an important role in radio frequency (RF) and microwave systems. Many applications using antennas can be found in the systems for wireless communications, energy harvesting, sensing network, and navigation. In 1886, Heinrich Hertz developed an experiment in which he forced a spark signal to occur in the gap of a dipole antenna. He then used a loop antenna as a receiver to capture the same spark signal. In 1901, Marconi was sending an information across the Atlantic Ocean. He used several vertical wires attached to ground as a transmit antenna and a 200-meter wire held up by a kit as a receive antenna. Based on Marconi's invention, early antenna technology was primarily focused on wire radiating elements with operating frequencies up to UHF. It was not until World War II that modern antenna technology was launched and new antenna structures such as waveguide apertures, horns and reflectors were largely used [1].

Microstrip antennas became popular in the 1970s primarily for spaceborne applications. Today they are often used for military and commercial applications. The microstrip antennas are usually with a metallic patch on a grounded substrate. Their advantages include low weight, small size, and ease of fabrication using printed-circuit technology, leading to the mainstream adoption of many wireless applications [2]. With increasing growth of mobile communications, the demand for miniature and low-profile antennas has brought microstrip antenna technology to the forefront.

A wide variety of waveguide couplers and power dividers were invented and characterized at the MIT Radiation Laboratory in the 1940s. These included E- plane and H-plane waveguide T-junctions, Bethe hole coupler, multi-hole directional couplers, Schwinger coupler, waveguide magic-T, and coaxial couplers. In the mid-1950s to the 1960s, many of the couplers were reinvented to use stripline or microstrip technology. The increasing use of planar structures also led to the development of new types of couplers and dividers, such as the coupled-line directional couplers [3]. Coupling between two transmission lines is introduced by their proximity to each other. Coupling such as crosstalk may be undesirable in high-speed circuits, but it is desirable in directional couplers for the purpose of power transfer from one line to the other.

## 1.2 Motivation

Recently, there has been a tremendous increase of research in microstrip antennas due to the development of communication and navigation systems. Various microstrip antennas with phase shifters have been presented [4]-[10]. Communication and navigation systems require a compact, practical, inexpensive and efficient antenna. In some researches, the communication systems use two antennas with different outputs to produce the signals with 90-degree phase difference. A high-frequency wireless system generally needs a low-loss antenna that was usually made with expensive substrate material. In addition, to obtain 90-degrees phase difference outputs, some works were done to integrate the antenna into the circuit of the system but it results in complicated fabrication. Another method uses a directional coupler, which is more efficient because it reduces the loss of the interconnection between the antenna and the circuit. Moreover, it is more practical with satisfactory performance because of the ease in design and fabrication of high performance microstrip antenna and directional coupler using low-cost print-circuit technology.

In this thesis, we introduced a microstrip antenna that operates from 5.5 to 5.8 GHz by integrating two feedlines within via holes, a circular patch and a reflector into the antenna. This antenna can obtain high gain with a compact size for navigation and communication applications. This antenna was further connected with a branch-line coupler for producing 90-degree phase difference outputs. This thesis provided a simple and effective method to design the microstrip antenna and branch-line coupler and then implemented them using easy fabrication process and low cost substrates.

## 1.3 Thesis Structure

This thesis focuses on designing and manufacturing microstrip antennas that can produce 90-degree phase-difference outputs with operating frequency from 5.5 to 5.8 GHz. An FR4 material with dielectric constant of 4.4 was used as the substrate of the antenna. Chapter 1 introduces the research background and motivation that initiate this study. Chapter 2 provides an overview of the theory and applications of microstrip antennas and directional couplers. Chapter 3 describes the details about the design and electrical properties of the microstrip antennas and branch-line couplers. This thesis elaborates the simulation and measurement results including the return loss, bandwidth, radiation pattern, polarization, gain, and efficiency of the presented antenna. Simulations were obtained using HFSS and ADS tools and fabrication of the antenna was done using etching process. Chapter 4 presents a summary of this thesis.

## 1.4 Objective

This thesis is based on research to develop the telecommunication equipment, especially for the wireless sensor network. Wireless sensor network has various types of one of them is the radar system at close range. One part of the main components in wireless network sensor network is an antenna. The implementation of antennas on the wireless sensor network system as the energy converter (signal power) from free space to the electrical device network system. In this research, the antenna that has been made and combined with branch line coupler that can produce 90 degrees different phase. this component device to be used on various types of configuration on the system wireless sensor network. Here are examples of the antennas used in combination with the branch line coupler: Quadrature radar with branch-line coupler, Radar with quadrature with the hybrid mixer, Self-Injection Locked Radar, Linear Polarization Continuously Sweeping Antenna, etc. From the previous examples have the different frequency and type of configuration. Therefore, the purpose of this thesis is an antenna model combined with a branch line coupler that has the frequency of 5.5 to 5.8 GHz with a one-antenna configuration type with two outputs.

# Chapter 2 RELATED THEORY

An antenna is a transitional structure between free-space and guiding device. The guiding device or transmission line may take the form of a coaxial line or a hollow pipe (waveguide), and it is used to transport electromagnetic energy from the transmitting source to the antenna, or from the antenna to the receiver. This research focuses on a microstrip antenna with a directional coupler for various wireless applications. Although the physical realization of the antenna may vary, the microstrip structure is common to all. This chapter is divided into several main topics about the basic concept of microstrip antenna and directional coupler.

## 2.1 Microstrip Lines

In this section, basic structure and design for microstrip lines, coupled microstrip lines, discontinuities, and components used for the design of microstrip antenna and directiomal coupler are briefly described. The general structure of a microstrip line is illustrated in Figure 2-1. A conducting strip (microstrip line) with a width $W$ and a thickness $t$ are on the top of a dielectric substrate that has a dielectric constant of $\varepsilon_r$ and a thickness of $h$, and the bottom of the substrate is a ground (conducting) plane.

This kind of elements presents a number of characteristics among those we can mention: the ground plane below the current conductor traces which helps to prevent the field excessive leakage and thus reduces radiation loss. The severity of the leakage depends on the relative dielectric constants *($\varepsilon_r$)* of the epoxy. A higher dielectric constant minimizes field leakage and cross-coupling [11].

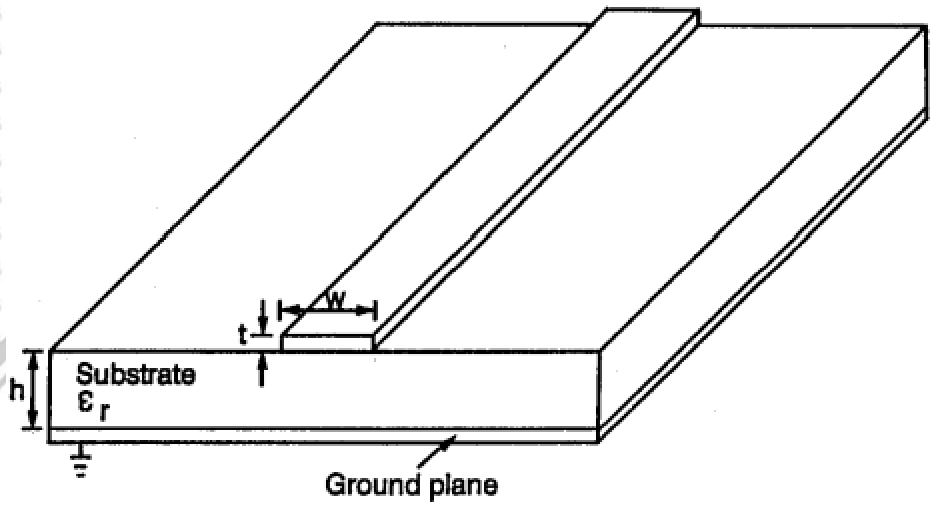


Figure 2-1 Microstrip line

## 2.2 Effective Dielectric Constant and Characteristic Impedance

Transmission characteristics of microstrip lines are described by two parameters, namely, the effective dielectric constant εr and characteristic impedance *Zc*, which may then be obtained by quasi-static analysis [12]. In quasi-static analysis, the fundamental mode of wave propagation in a microstrip line is assumed to be pure TEM. The above two parameters of microstrip line are then determined as follows

$$\varepsilon_{re} = \frac{C_d}{C_a} \quad \text{(Eqn.2-1)}$$

$$Z_c = \frac{1}{c\sqrt{C_a C_d}} \quad \text{(Eqn.2-2)}$$

Where *Cd* is the capacitance per unit length with respect to the substrate, *Ca* is the capacitance per unit length with the respect to air, and *c* is the velocity of electromagnetic waves in free space *(c=3.0 × 108 m/s).*

This section describes the materials used for antenna construction. The characteristic of materials have several crucial parameters. One of them is $\varepsilon_r$. Mathematically, $\varepsilon_r$ is very influential to antenna design and measurement results so we need to choose $\varepsilon_r$ carefully. For example, we determine $\varepsilon_r$ to obtain the expected antenna size and the impedance matching to appropriate level.

## 2.3 Coupled Resonator Circuits

In general, the coupling coefficient of coupled RF/microwave resonators, which can be different in structure and can have different self-resonant frequencies (see Figure 2-2), may be defined on the basis of the ratio of coupled energy to stored energy

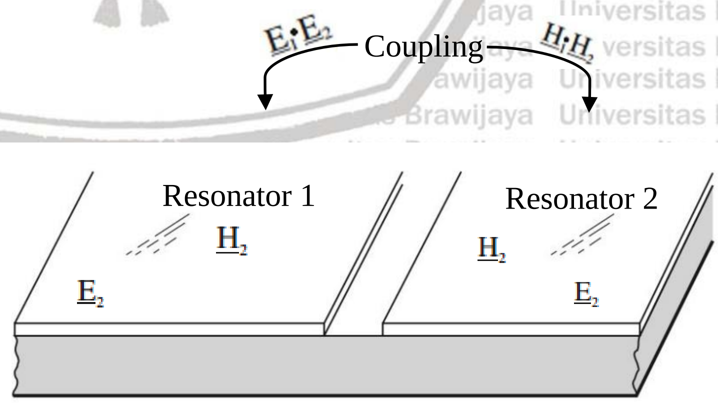


Figure 2-2 General coupled RF/microwave resonators where resonators 1 and 2 can be different in structure and have different resonant frequencies.

It may be easier by using full-wave EM simulation or experiment to find some characteristic frequencies that are associated with the coupling of coupled RF/microwave resonators. The coupling coefficient can then be determined based on the physical structure of coupled resonators if the relationship between the coupling coefficient and the characteristic frequencies is established. In what follows, we derive the formulation of such relationships. In this study, we use the theory to design the coupled resonator circuit using the parameters generated on antennas and couple circuits.

## 2.4. Antenna

Antenna is a very important component to support wireless communication system because the antenna can radiate and receive electromagnetic waves which contain information signal. In addition, the antenna is a transitional device between free space and transmission line. A transmission-line Thevenin equivalent of the antenna system in the transmitting mode is shown in Figure 2-3. The source is represented by an ideal generator, the transmission line is represented by a line with characteristic impedance Zc, and the antenna is represented by a load ZA [ZA = (RL + Rr) + jXA] connected to the transmission line.

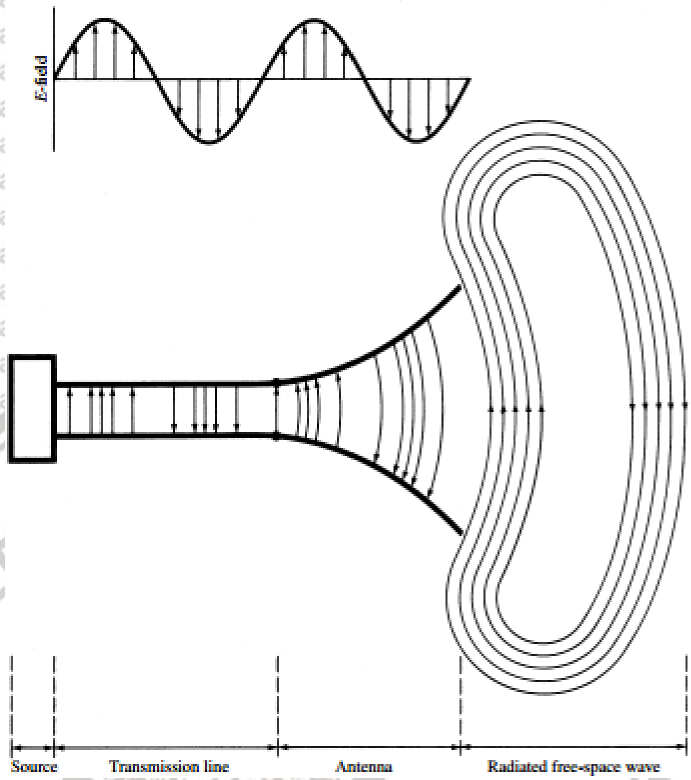


Figure 2-3 Antenna as a transition device

To describe the performance of an antenna, it is necessary to understand the key antenna parameters [1]. They include the antenna terminal impedance, VSWR, RL, bandwidth, radiation pattern, polarization, directivity, and gain.

## 2.5 Antenna Parameters

To explain the performance of an antenna, it is necessary to understand the parameters of the antenna. The antenna parameters are important to explain the performance of an antenna. This thesis introduces how to obtain the antenna parameters using simulation and measurement.

### 2.5.1 Impedance Terminal

The antenna terminal impedance needs to be known, for the purpose of transferring power from or to the antenna. In general, the antenna terminal impedance is defined as the impedance generated by the antenna terminal or the ratio between the voltage to the current on the terminal, as written by [1]:

$$Z_A = R_A + jX_A \quad \text{(Eqn. 2-3)}$$

The total power supplied to the antenna is

$$P_{in} = I^2.R_A \quad \text{(Eqn. 2-4)}$$

With the emitted power given by

$$P_{rad} = I^2.R_{rad} \quad \text{(Eqn. 2-5)}$$

While the antenna impedance can be obtained from the reflection coefficient with the following equation:

$$|\Gamma| = \left|\frac{Z_{ant} - Z_c}{Z_{ant} + Z_c}\right| \quad \text{(Eqn.2-6)}$$

So, the antenna impedance can be obtained as

$$Z_{ant} = Z_c\left(\frac{1+|\Gamma|}{1-|\Gamma|}\right) \quad \text{(Eqn. 2-7)}$$

### 2.5.2 Return Loss/S-Parameter

Return loss (RL) is the power lost due to reflection. RL is caused by the impedance mismatch between the antenna and the load. The reflection coefficient is the ratio between the reflected voltage and the forward voltage. A good antenna has a return loss above 10 dB, that is, 90% of the signal is delivered to the load, and 10% is reflected [13]. The reflection coefficient and return loss are defined as

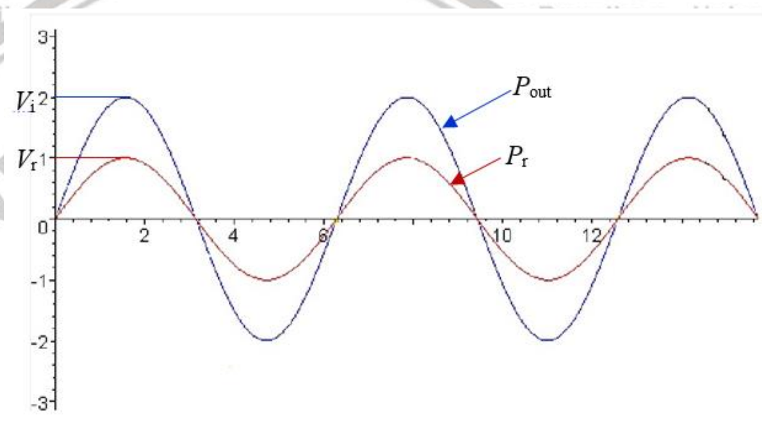


Figure 2-4 Amplitude of the forward wave and reflected wave

$$\Gamma = \frac{V_r}{V_i} \quad \text{(Eqn. 2-8)}$$

$$RL = -20 \cdot \log \Gamma \quad (dB) \quad \text{(Eqn. 2-9)}$$

For impedance match between the load and the antenna, $\Gamma = 0$ and $RL = \infty$ which means no power is reflected. If $|\Gamma| = 1$ and $RL = 0\ dB$, then all power is reflected.

### 2.5.3 VSWR(Voltage Standing Wave Ratio)

An antenna VSWR is the ratio between the amount of incoming voltage and reflected voltage and the difference between the incoming voltage and the reflected voltage. The VSWR can be obtained from the reflection coefficient with the following equation [14]:

$$VSWR = \frac{1+|\Gamma|}{1-|\Gamma|} \quad \text{(Eqn. 2-10)}$$

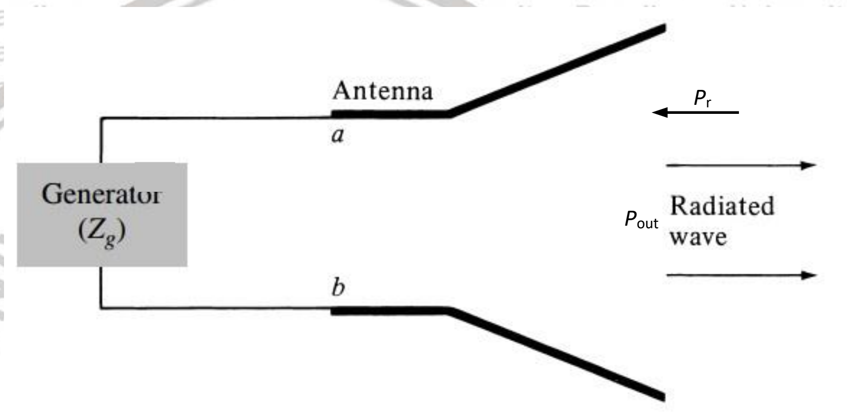


Figure 2-5 Antenna in transmission mode

Γ can be obtained from the equation:

$$Pr = |\Gamma|^2 \cdot P_{out} \quad \text{(Eqn. 2-11)}$$

$$\Gamma^2 = \frac{P_r}{P_{out}} \quad \text{(Eqn. 2-12)}$$

**2.5.4 Polarization**

Polarization is one of the antenna parameters described in the radiated electric field direction. Polarization can also be interpreted as the vector direction of an EM wave or in a more precise language is the direction of the EM waves electric field generated by an antenna. The polarization is defined for a transmitted wave or a received wave via an antenna in a particular direction. Polarization can be classified as linear, circular or ellipitcal. If the EM wave is a vector field, then the vector field is described by the electric field as a function of time. If the wave field is aligned along a straight line, it is then said to be linearly polarized [1].

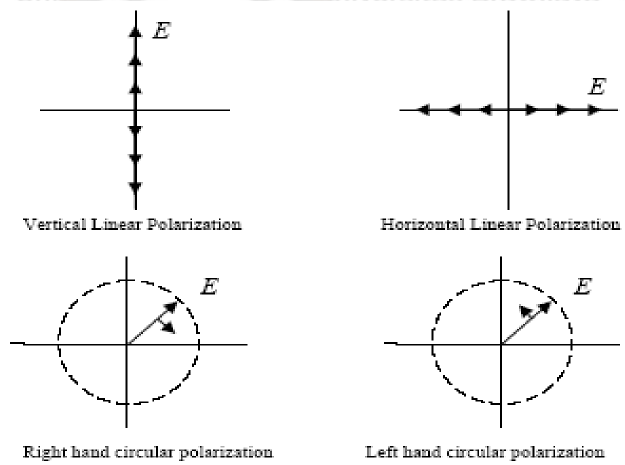


Figure 2-6 The general form of polarization

In general, the electric field of the antenna (E-field) has two components in a transverse plane. The two components of *E* field might have different magnitudes and angular directions. Both antennas on the transmitter and the receiver side must have the same polarization to obtain that the transmitted wave is maximally received by the antenna receiver. If the two linearly polarized antennas are not in the same orientation, then the received energy will be decreased due to polarization mismatch. Linear polarization has two forms, i.e., linear horizontal polarization and linear vertical polarization.

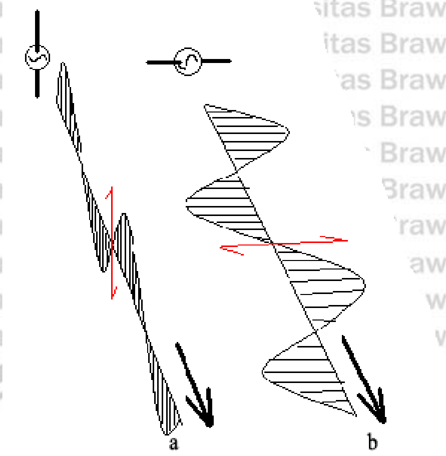


Figure 2-7 The Waves with linear polarization: (a) vertical, (b) horizontal

### 2.5.5 Radiation Pattern

The antenna radiation pattern is defined as a graphical illustration of the properties of far-field radiation from the antenna as a function of space coordinates (three dimensions). The properties of radiation include radiation intensity, field strength, and polarization. The antenna characteristics such as beamwidth and front-to-back ratio *(F/B)* can be determined if the radiation pattern is known.

Based on the radiation pattern, the antenna can be classified into several types, they are isotropic, directional, and omnidirectional. The isotropic radiator is defined as a lossless antenna that has the same radiation in all directions. Although this pattern is an ideal pattern that is physically impossible to realize. It is often used as a reference. Directional antennas have more effective radiation in a particular direction than other directions. While omnidirectional antenna is an antenna that has a directional pattern on the vertical plane and non-directional pattern on the horizontal planes.

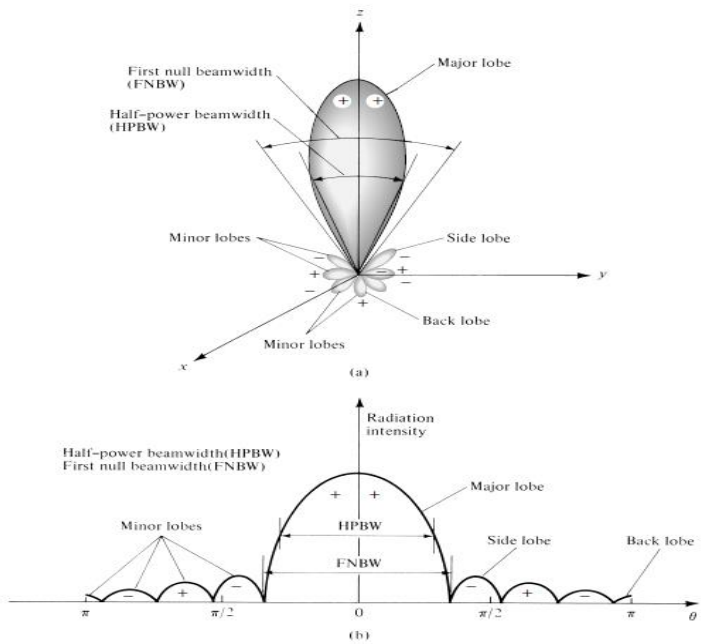


Figure 2-8 (a) Antenna Radiation Pattern, (b) Antenna Radiation Pattern in Cartesian Coordinate

Radiation pattern from 0$^{o}$ to 360$^{o}$ is usually plotted as a polar graph. Then the -3 dB (half power) beamwidth can be found in both horizontal and vertical radiation patterns. The radiation pattern can be measured by moving the antenna probe around the antenna at a fixed distance, then record the response as a function of angular coordinates ($\theta$,$\phi$) at a constant radius [1].

### 2.5.5 Antenna Gain

One of the most important measurements to describe antenna performance is gain. The gain of the antenna means the ratio of power emitted by a specific antenna compared to the power emitted by an isotropic antenna. Although the antenna gain is closely related to directivity, it additionally includes the information of antenna efficiency. The gain antenna is classified into absolute gain and relative gain. To understand both gain definitions, we can refer to Figure 2-9 as follows.

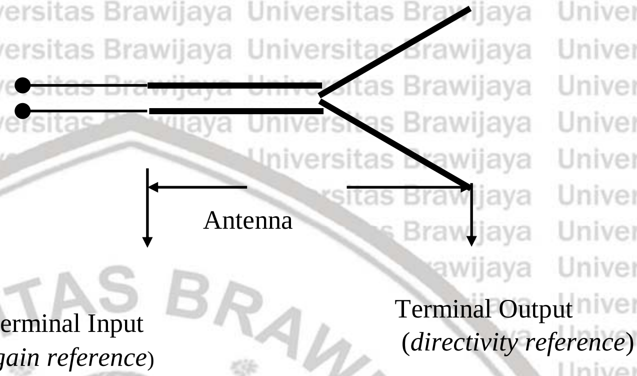


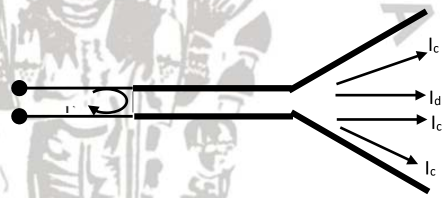


Figure 2-9 The reference terminals and antenna losses

The absolute gain of an antenna (in a particular direction) is defined as the ratio of the radiation intensity in a particular direction to the radiation intensity that is obtained as the antenna is radiated isotropically. The radiation intensity of an isotropically radiated antenna is equal to the received power (at the input terminal) of the antenna divided by 4π. Thus, the absolute gain is expressed as

$$G = 10 \cdot \log \frac{4\pi \cdot U_m}{P_{in}} \text{ (dB)} \qquad \text{(Eqn. 2-13)}$$

The relative gain of an antenna is the ratio of radiated power in a particular direction to that of the reference antenna in a reference direction (note that both antennas have the same input power). For relative gain, the reference antenna uses an isotropic antenna without loss. That is

$$G = \frac{4\pi I(\theta,\phi)}{P_{in}\,(\text{lossless isotropic source})} \quad \text{(Eqn. 2-14)}$$

The relative gain indicates the power emitted by a particular antenna compared to that emitted by an isotropic antenna with a spherical radiation pattern. The isotropic radiator is actually a theoretical concept, while in practice the antenna gain is usually compared to the radiation intensity of a standard ½ λ dipole antenna whose gain is approximately 1.64 times or 2.15 dB larger than an isotropic radiator. So the relative gain can be expressed as [1]:

$$\mathrm{G} = 1.64 \times \frac{\mathrm{P_u}}{\mathrm{P_r}} \quad \text{(Eqn. 2-15)}$$

$$G(dB) = 10 \log 1.64 \frac{\mathrm{P_u}}{\mathrm{P_r}} \quad \text{(Eqn. 2-16)}$$

$$\mathrm{G} = 2.15 + \mathrm{P_u(dBm)} - \mathrm{P_r(dBm)} \quad \text{(Eqn. 2-17)}$$

## 2.6 Microstrip Antenna

Microstrip antenna is an antenna that is made of a conductor element (a radiating element) and placed above the ground plane where there is a dielectric material between them. Microstrip antennas have advantages including light weight, small size, and single- or multi-band operation with circular or linear polarization. However, microstrip antennas also have shortcomings such as narrow bandwidth, small gain, and low efficiency.

In microstrip antennas, there are four fundamental components including patch (radiating element), dielectric substrate, feed and ground.

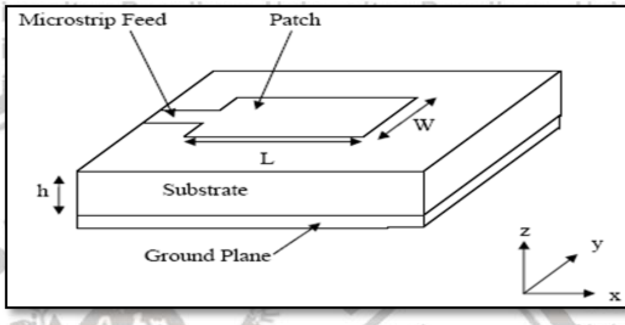


Figure 2-10 Microstrip antenna

Patch is a radiating element in a microstrip antenna. It is a metal sheet on the dielectric substrate. Some patch shapes of microstrip antenna can be seen in Figure 2-10. Every patch shape has its own characteristics [1].

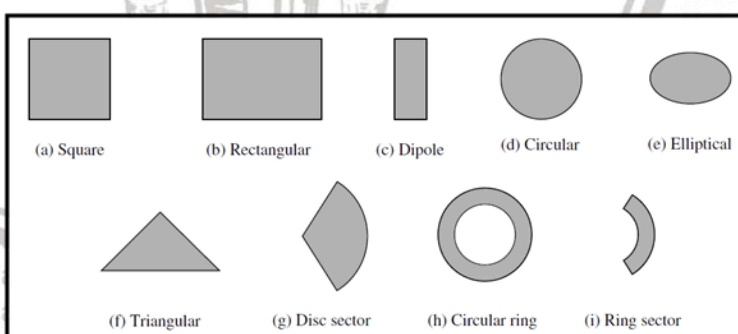


Figure 2-11 The patch shape of microstrip antenna

The dielectric substrate is located between patch and ground. Each substrate has a dielectric constant ($\varepsilon_r$) that typically ranges from 2.2 to 12 with a thickness that typically ranges around $0{,}003\lambda_0 \le h \le 0{,}05\lambda_0$. The selection of substrate is influential to the antenna performance. If the substrate is thicker or the dielectric constant is smaller, the radiation efficiency and bandwidth increase but the antenna dimension also increases [1].

Feed is a used to connect a microstrip antenna to the circuit. The ground plane is a metallic material on the bottom side of the dielectric substrate that functions as a reflector.

To determine the dimensions of the radiating element, we need to know the operating frequency *(fr)* in terms of the wavelength of free space *($\lambda_0$)*

$$\lambda_0 = \frac{c}{f_r} \qquad \text{(Eqn. 2-18)}$$

After $\lambda_0$ is known, the wavelength of microstrip transmission line *($\lambda_d$)* can be found by the following equation:

$$\lambda_d = \frac{\lambda_0}{\sqrt{\varepsilon_r}} \qquad \text{(Eqn. 2-19)}$$

### 2.6.1 Radiating Element Dimension

To find the width of a radiating element of rectangular shape *(W)*, the following equation can be used:

$$W = \frac{c}{2 \cdot f_r} \sqrt{\frac{2}{\varepsilon_r + 1}} \qquad \text{(Eqn. 2-20)}$$

Meanwhile, to find the length of the radiating element *(L)*, we need to calculate the effective dielectric constant using the following equation:

$$\varepsilon_{reff} = \frac{\varepsilon_r + 1}{2} + \frac{\varepsilon_r - 1}{2}\left[1 + 12\frac{h}{W}\right]^{-\frac{1}{2}} \qquad \text{(Eqn. 2-21)}$$

Thus, the length of the radiating element *(L)* can be expressed by the following equation :

$$L = \frac{c}{2 \cdot f_r \sqrt{\varepsilon_{reff}}} - 2 \cdot \Delta L \qquad \text{(Eqn. 2-22)}$$

where

$$\Delta L = 0.412 \cdot h \cdot \frac{(\varepsilon_{reff}+0.3)\left(\frac{W}{h}+0.264\right)}{(\varepsilon_{reff}-0.258)\left(\frac{W}{h}+0.8\right)} \qquad \text{(Eqn. 2-23)}$$

To find the radius of a radiating element of circular shape, the following equation can be used [1]:

$$a = \frac{F}{\left\{1+\frac{2h}{\pi\varepsilon_r F}\left[ln\left(\frac{\pi F}{2h}\right)+1.77726\right]\right\}^{\frac{1}{2}}} \qquad \text{(Eqn. 2-24)}$$

where the function *(F)* is given by

$$F = \frac{0.8791\times 10^{9}}{j} \qquad \text{(Eqn. 2-25)}$$

### 2.6.2 Feedline Dimension

To calculate the width of microstrip line, the following equation can be used:

$$W_0 = \frac{k}{Z_0} \times \frac{h}{\sqrt{\varepsilon_r}} \qquad \text{(Eqn. 2-26)}$$

Then the length of the transmission line can be calculated by

$$L_o = \frac{1}{4}\lambda_d \qquad \text{(Eqn. 2-27)}$$

The length of inset feed can be found by the following equations [15] :

- Rectangular radiating element

$$R_{in}(y = y_o) = R_{in}(y = 0)\cos^2\left(\frac{\pi}{L}y_0\right) \quad \text{(Eqn. 2-28)}$$

- Circular radiating element

$$y_0 = 0.3d \quad \text{(Eqn. 2-29)}$$

The distance between the radiating elements is

$$r \geq 0.6\lambda_d \quad \text{(Eqn. 2-30)}$$

## 2.7 Directional Couplers

A directional coupler is a passive device which couples part of the input power to another port. The two transmission lines are set close enough to pass and couple the energy from one port to another. As shown in Figure 2-11, the device has four ports: input port, through port, coupled port and isolated port. A directional coupler is a four port network to divide the power of the input port into the through and coupled ports, while the isolated port is terminated with a matched load (typically 50 ohms). It should be pointed out that since the directional coupler is a symmetrical reciprocal device, any port can serve as the input port while the directly connected port is the through port; the adjacent port is the coupled port, and the diagonal port is the isolated port [16].

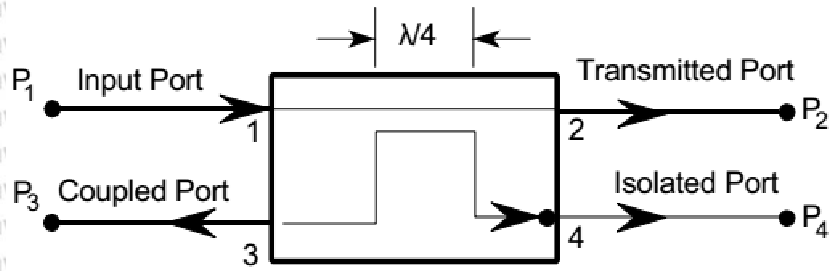


Figure 2-12 Directional Coupler

Directional couplers can be designed for arbitrary power division, while hybrid junctions usually have equal power division. Hybrid junctions have either a 90◦ or 180◦ phase difference between the output ports. When the output power of the coupled port is half the power of the input port (i.e. 3 dB below the input power), the output power of the through port is also 3 dB below the input power and equals that of the coupled port. For coaxial couplers, the frequency range of the coupling factor is usually specified by the manufacturers. The through factor response covers a wider frequency range (e.g., if the specified frequency range of the coupling factor is 2-4 GHz, the available frequency range of the through factor may cover from 1 to 5 GHz - see Figure 3). However, it should be noted that the coupler's response is periodic with frequency.

## 2.8 The Quadrature (90◦) Hybrid

A directional coupler is a four-port network for power division. It is commonly used in microwave systems or telecommunication devices. Quadrature hybrids are 3 dB directional couplers with a 90◦ phase difference between the outputs of the through and coupled ports. These hybrids are often made with microstrip lines and also known as branch-line couplers. Other 3-dB couplers, such as coupled-line couplers, can also be used as quadrature couplers. Besides these, waveguide couplers can also be used but they are bulky. The phase difference between two output S parameters is 90 degrees for an even number of slots but deviates from 90 degrees for an odd number of slots. However, it tends to approach 90 degrees as the number of slots and the coupling factor increase. Its scattering matrix is expressed as [12]:

$$[S] = \frac{-1}{\sqrt{2}} \begin{bmatrix} 0 & j & 1 & 0 \\ j & 0 & 0 & 1 \\ 1 & 0 & 0 & j \\ 0 & 1 & j & 0 \end{bmatrix} \quad \text{(Eqn. 2-31)}$$

The use of a pair of slots repeated n times at λ/4 intervals along the common broad wall of parallel waveguides can be designed to have perfect directivity at a selected frequency f0, and have flat coupling at this frequency. With additional such pairs spaced λ /4 along the waveguides, the coupling can be increased while the bandwidth for high directivity also increases. The branch-line hybrid also has the advantage that it may be realized using slots in the ground plane of a microstrip circuit. It is observed that the branch-line hybrid has a high degree of symmetry, so any port can be used as the input port. The output ports are on the opposite side of the junction to the input port, and the isolated port is the remaining port on the same side of the input port. This symmetry is also indicated in the scattering matrix because each row of the scattering matrix can be obtained as a transposition of the first row.

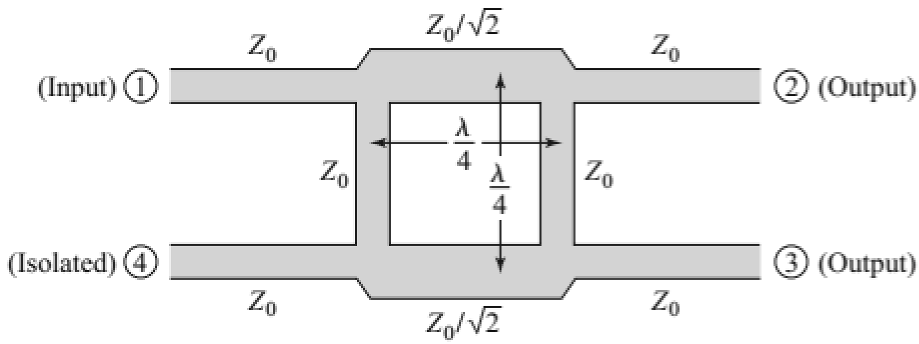


Figure 2-13 Geometry of a branch-line coupler

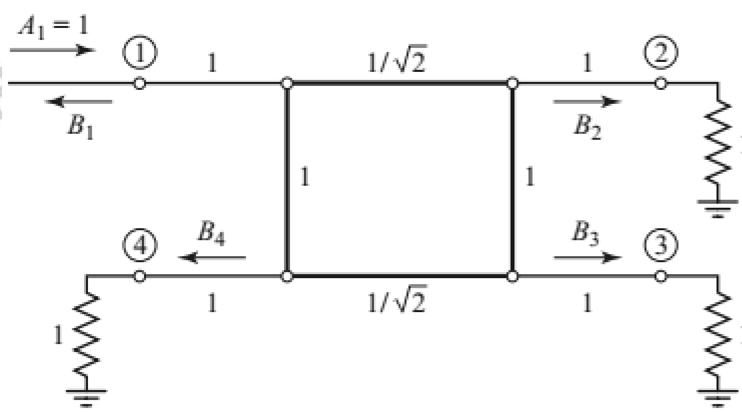


Figure 2-14 Diagram of the branch-line coupler with normalized loads

As shown in Figures 2-15 and 2-16, a λ / 4 transmission line in the branch-line coupler can be represented by a π-equivalent network composed of a series inductor and two capacitors [18]. The element values are determined using the following equations [19].

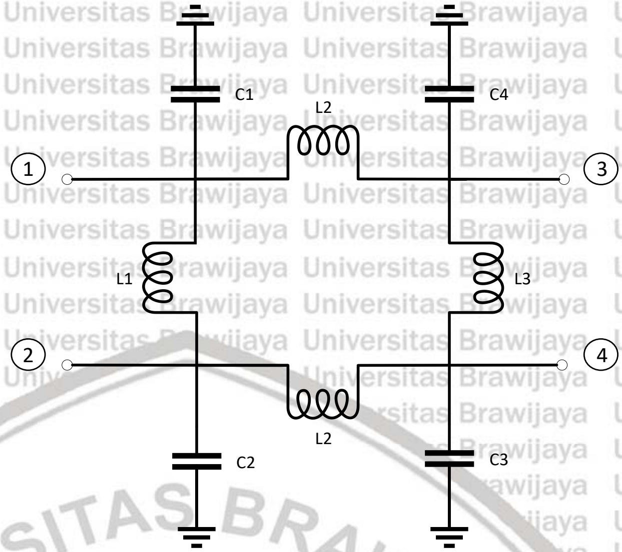


Figure 2-15 Lumped-element equivalent circuit of the branch-line directional coupler

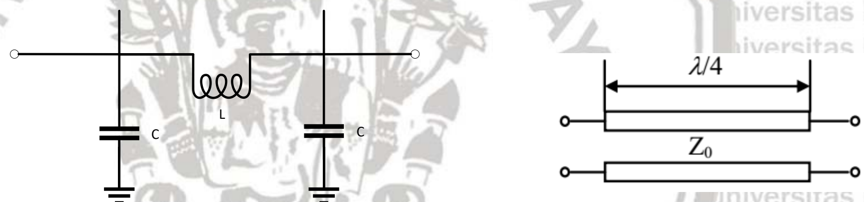


(a) π-equivalent network (b) λ/4 coupled line

Figure 2-16 π-equivalent network and λ/4 coupled line

$$A_z = \begin{bmatrix} 0 & jZ \\ j\frac{1}{Z} & 0 \end{bmatrix} \quad \text{(Eqn.2-32)}$$

$$A_{LC} = \begin{bmatrix} 1+\frac{L}{C} & j2\pi f_0 L \\ -j\frac{1}{j2\pi f_0 C}\left(2-\frac{L}{C}\right) & 1+\frac{L}{C} \end{bmatrix} \quad \text{(Eqn.2-33)}$$

where AZ and ALC are the ABCD matrix of the λ/4 transmission line and the LC equivalent network, respectively. By comparing these two matrices, the element values in the equivalent network can be obtained. Notably, L1, L2, and L3 indicate the series inductors of the branch and main lines while C1 and C2 are the shunt capacitors of the branch and main lines. Their values are given by [20] :

$$L_1 = \frac{Z_0}{2\pi f_0} \quad \text{(Eqn.2-34)}$$

$$L_2 = \frac{\sqrt{2R}Z_0}{4\pi f_0} \quad \text{(Eqn.2-35)}$$

$$L_3 = \frac{RZ_0}{2\pi f_0} \quad \text{(Eqn.2-36)}$$

$$C_1 = \frac{1}{2\pi f_0 Z_0}\left(1 + \sqrt{\frac{2}{R}}\right) \quad \text{(Eqn.2-37)}$$

$$C_2 = \frac{1}{2\pi f_0 Z_0}\left(\frac{1}{R} + \sqrt{\frac{2}{R}}\right) \quad \text{(Eqn.2-38)}$$

From the analysis above, the lumped-element equivalent circuit can be established. With knowledge of the load impedance ZL, the equivalent-circuit elements are computed using Eqn.2-32 - Eqn.2-38.

# Chapter 3 DESIGN AND EXPERIMENT

## 3.1 Experimental Setup

The procedure of designing and implementing microstrip antenna and branch-line coupler in this thesis is shown in the following flowchart:

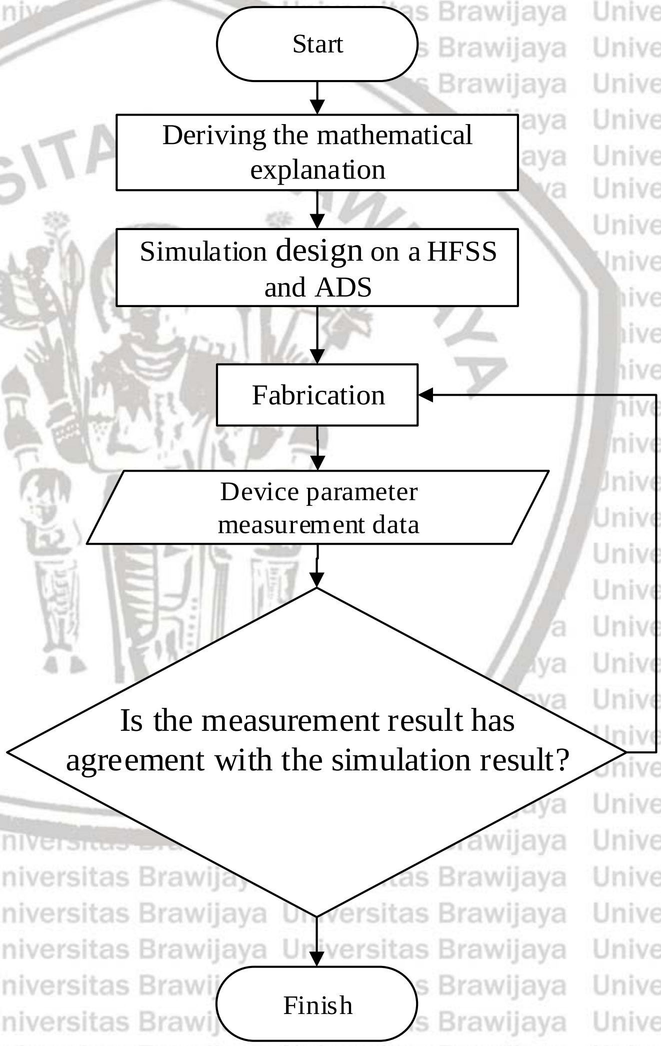


Figure 3-1 Flowchart of the research

This section explains the design of microstrip circular patch antenna. This microstrip antenna is excited using microstrip line feed. The design is a simple, easy to implement and can generate the desired parameters to meet the required specifications. There are several steps to design this antenna, including the selection of the substrate, the type of antenna and the use of the transmission line. After that, it is simulated with HFSS and ADS to obtain the antenna parameters. If the simulated antenna parameters results are not good, the optimization process is used to for further improvement.

## 3.2 Design of Microstrip Antenna on FR-4 Substrate

The microstrip antenna was analyzed mathematically based on the literature study. The design also relies on the EM software tool to find out the antenna parameters. Design steps and antenna simulations are important to see if the simulation results meet the predetermined specifications. Design of microstrip antenna needs to know about the substrate to be used. The parameters of the substrate materials used in this study are as follows:

Fiberglass Epoxy Material - FR4

The dielectric constant *($\varepsilon_r$)* = 4.4

Dielectric thickness *(h)* = 0.0018 m = 1.8 mm

Loss tangent *(tan δ)* = 0.018

Copper substrate (conductor) coating material:

The thickness of the conductor material (*t*) = 0.0001 m

The conductivity of copper (*σ*) = $5.80 \times 10^7$ mho $m^{-1}$

The characteristic impedance of channel ($Z_0$) = 50 Ω

The specifications of the antenna specification are

Operating frequency range : 5.5 GHz - 5.8GHz

VSWR : < 2

Gain :> 3 dB

Return Loss : < -15 dB

## 3.3 Microstrip Antenna Dimension Design

Calculations used to determine the dimensions of the antenna can be viewed in the following flowchart :

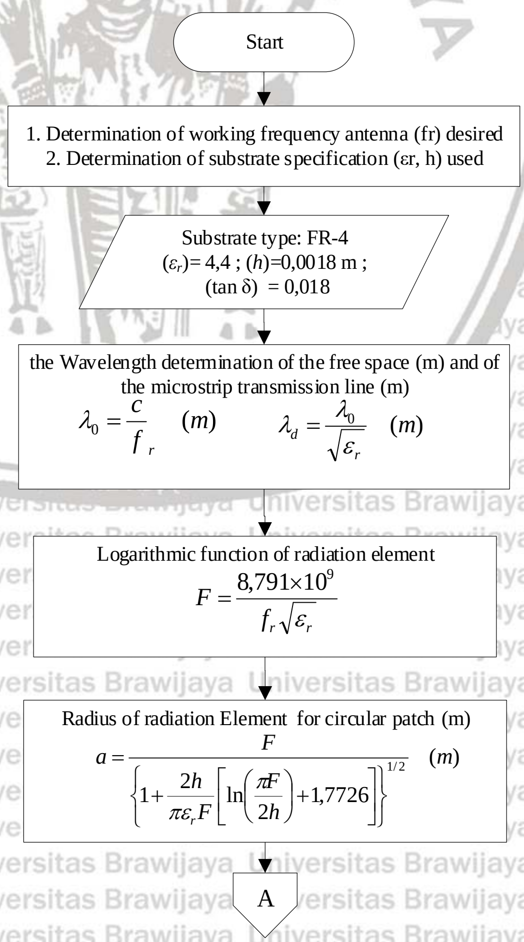

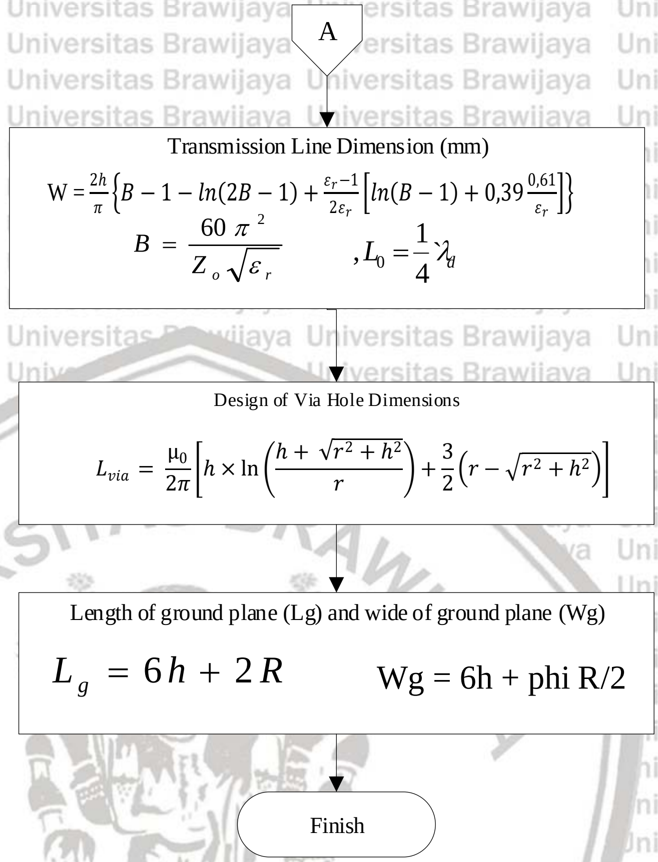


Figure 3-2 Design process of antenna dimension

### 3.3.1 Radiating Elements

Before determining the dimension of radiating element, it must determine the resonance frequency (fr) first. The resonant frequency of the microstrip antenna is the center frequency of the operating frequency range 5.5-5.8GHz, that is 5.65 GHz, and the propagation velocity in free space (c) is $3 \times 10^8$ m / s.

The wavelength of microstrip transmission line is 0.025313 m. The dielectric constant influences the electromagnetic waves traveling in the material. The high dielectric constant makes the propagation delay in the material larger. This means that the propagation velocity is slower or the propagation wavelength is shorter.

### 3.3.2 Circular Patch

The microstrip antenna includes two rectangular radiating elements that are connected with via holes to a larger circular radiating element (circular patch), so this antenna basically uses the circular patch as the main radiating element. The radius of the circular patch can be determined using equation 2-24 [1].

First, calculate the function F. With $h$ = 0.8mm; $f$r = 5.65 GHz; (εr) = 4.4, the function F can be calculated as 0.74176 according to equation 2-25. Then substitute these values into the formula regarding the dimension of the circular patch. So the radius of the circular patch is determined as 7.3593 mm.

### 3.3.3 Ground Plane

To calculate the length and width of the ground plane, the following equations can be used [13]:

$$L_g = 6h + 2R \quad \text{(Eqn.3-1)}$$

$$W_g = 6h + \frac{\pi}{2}R \quad \text{(Eqn.3-2)}$$

where R is the radius of the circular patch. Then we can calculate the length of the ground plane as 25.59 mm and the width of the ground plane as 22.41 mm. Based on the calculation, the dimension of the ground plane is determined as 25.59 mm × 22.41 mm.

### 3.3.4 Via Hole

Via hole is a conductor that connects the different planar conducting elements in the substrate. The inductance of the via hole can be estimated using [17]:

$$L_{via} = \frac{\mu_0}{2\pi}\left[h \times \ln\left(\frac{h+\sqrt{r^2+h^2}}{r}\right) + \frac{3}{2}\left(r - \sqrt{r^2+h^2}\right)\right] \quad \text{(Eqn.3-4)}$$

where r is the radius of via hole and h is the thickness of the substrate. The formula above represents an empirical factor change of the second term from 1 to 3/2. The following relationship may be used as a close approximation to the via hole resistance and is valid independent of the ratio of metalization thickness to skin depth.

$$R_{via} = R_{dc}\sqrt{1+\frac{f}{f_\delta}} \quad \text{(Eqn.3-5)}$$

$$f_\delta = \frac{1}{\pi\mu_0\sigma t^2} \quad \text{(Eqn.3-6)}$$

With the above formula, the radius of the via hole is determined as 0.3 mm.

### 3.3.5 Transmission Line

To calculate the dimensions of the transmission-line feed using Eqn.3-8 where the parameter B is defined as

$$B = \frac{60\pi^2}{Z_0\sqrt{\varepsilon_r}} \quad \text{(Eqn.3-7)}$$

The B is calculated as 5.4045 according to Eqn.3-7. Then the width of the microstrip line can be obtained using [1]:

$$W = \frac{2h}{\pi}\left\{B - 1 - ln(2B-1) + \frac{\varepsilon_r - 1}{2\varepsilon_r}\left[ln(B-1) + 0{,}39 - \frac{0{,}61}{\varepsilon_r}\right]\right\} \quad \text{(Eqn.3-8)}$$

As a result of calculation, W is obtained 0.73947 mm. The length of microstrip line is calculated using Eqn.2-27 and obtained as 6.3275 mm.

## 3.4 Branch-Line Coupler

To determine the dimension of the microstrip lines used in a branch-line coupler, firstly it must determine the resonance frequency (fr), the wavelength, the impedance of each port and the substrate material to be used. The resonant frequency of coupler is consistent with the antenna. That is 5.65 GHz and the microstrip lines used in the branch-line coupler are ¼ λ. The coupler has four ports. Each port has a 50 ohm characteristic impedance. The substrate material used is the same as that of the antenna, which is an FR4 substrate with $\varepsilon_r = 4.4$ and $\sigma = 5.8e7$. The 90 degree hybrid design is based on a branch-line coupler. In a branch-line coupler as shown in Figure 3-3, there are two inputs and two outputs. In addition, the microstrip lines of the coupler have two different impedances. One is 50 ohm and the other is 50/√2 Ω. To obtain the dimension of these microstrip lines, the following parameter need to be calculated in advance [2]:

$$A = \frac{Z_0}{60}\sqrt{\frac{\varepsilon_r+1}{2}} + \frac{\varepsilon_r-1}{\varepsilon_r+1}\left(0.23 + \frac{0.11}{\varepsilon_r}\right) \qquad \text{(Eqn.3-9)}$$

A is calculated as 1.5298 for a 50 Ω microstrip line and 1.1288 for a 50 /√2 Ω microstrip line. Then the width of the microstrip lines can be estimated by

$$W = \frac{8e^A}{e^{2A}-2}\,h \qquad \text{(Eqn.3-10)}$$

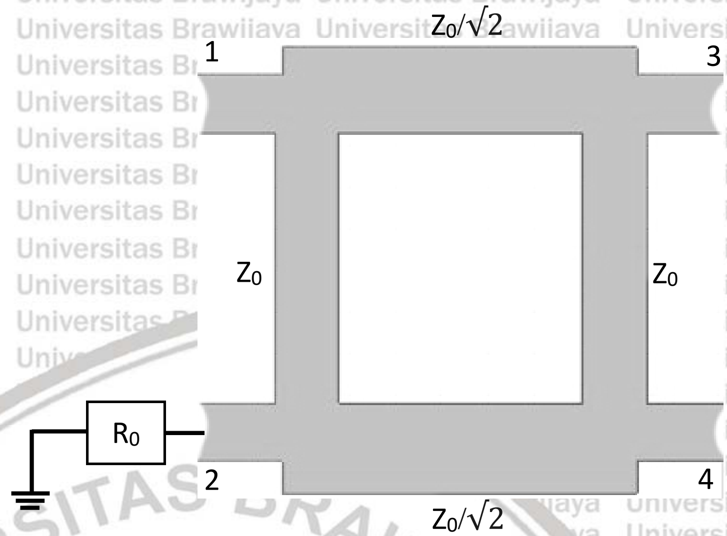


Figure 3-3 The branch-line coupler

According to Eqn.3-10, W is calculated as 1.5294 for a 50 Ω microstrip line and 3.2718 for a 50/√2 Ω microstrip line. The length of these microstrip lines is set as 1/4 λ to obtain 90 degree phase difference between the two outputs.

## 3.5 Simulation and Optimization

The final design of the microstrip antenna and branch-line coupler in this thesis was done with the help of EM simulation and optimization. This section shows how the final design was achieved.

### 3.5.1 Microstrip Antenna

Design of microstrip antenna was carried out mathematically based on the study in the literature. The design results were then used in an HFSS to perform the optimization for the antenna parameters. The antenna simulation process is important to see whether the design results meet the predetermined specfications or not. After that, we obtain the dimension of the patch, ground plane and transmission-line feed. The first parameter that want to observe is the return loss to check the impedance mismatch of the antenna. The following explains the designed microstrip antenna structure.

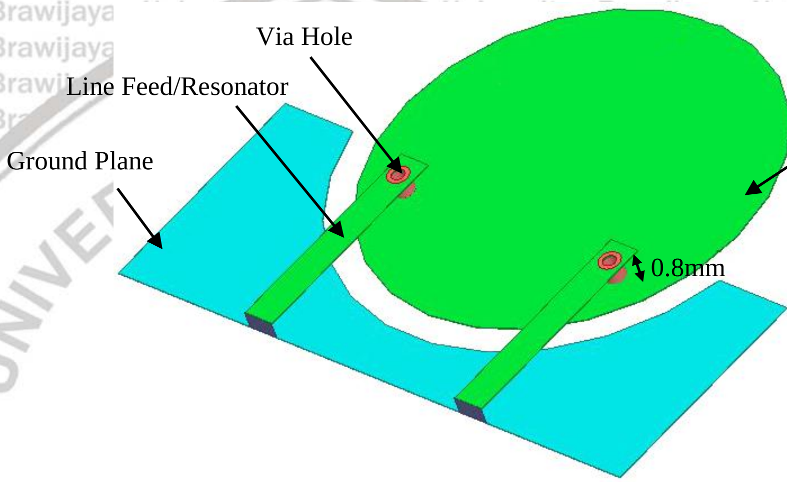


Figure 3-4 Microstrip antenna structure

Figure 3-4 shows the proposed design of the microstrip antenna. The design has two same size feedlines that are connected to the circular patch with via holes. These two feedlines are terminated with 50 ohm load impedance in the simulation. This antenna uses an FR4 substrate with a thickness of 0.8 mm, as shown in Figure 3-5. Notably, the conductor thickness is 0.035 mm.

In the simulation, the antenna design also tries different substrate materials. Moreover, as shown in Figure 3-6, it was found that adding a reflector below the antenna is useful to increase the gain and directivity of the antenna.

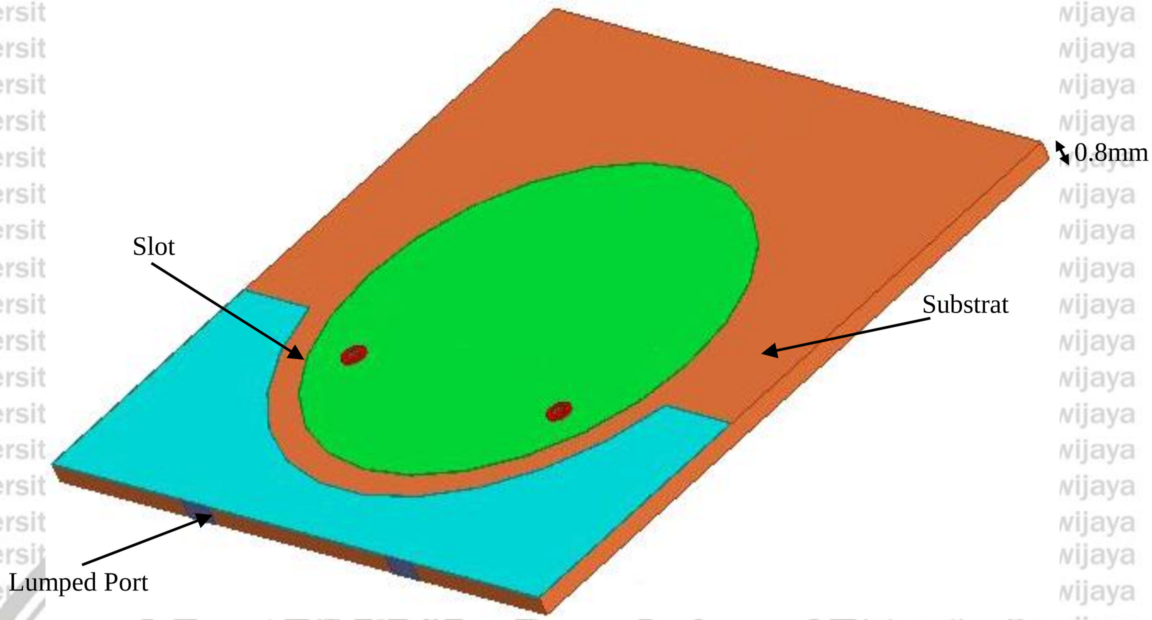


Figure 3-5 Design of microstrip antenna

The things that need to be done after setting the simulation parameters based on the theory are to perform the optimization to meet all the predetermined antenna specifications. Optimization can be repeated until the desired specifications are achieved. Optimization was done by altering the dimensions of each part of the antenna to link the changes to each specification. As a result, the antenna dimensions after optimization are shown in Table 3-1 by referring to Figure 3-7.

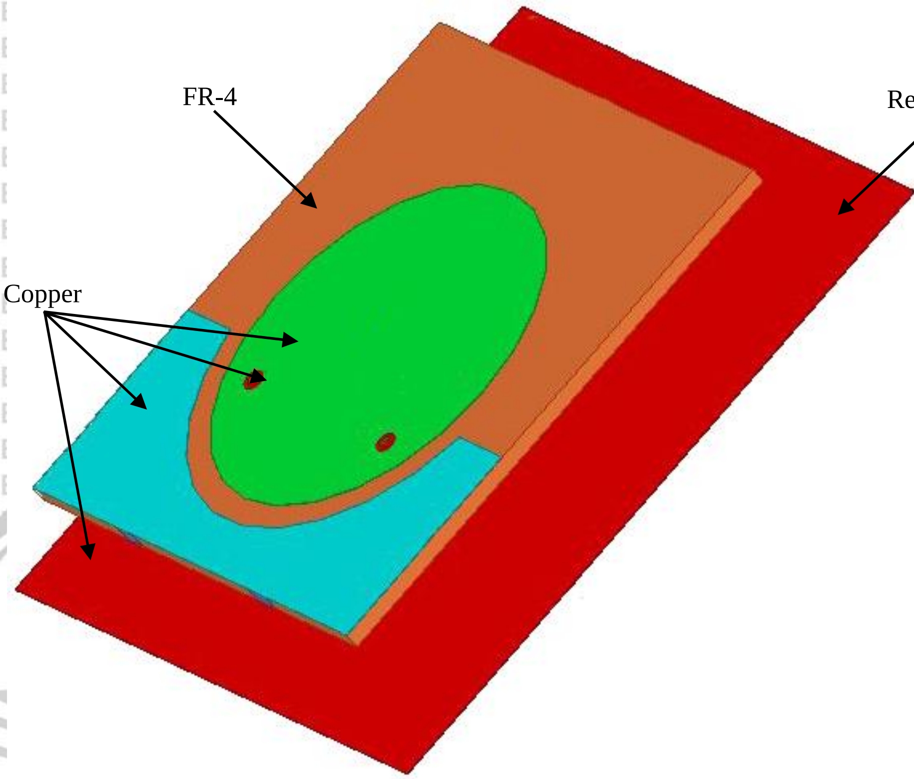


Figure 3-6 Microstrip antenna with a reflector

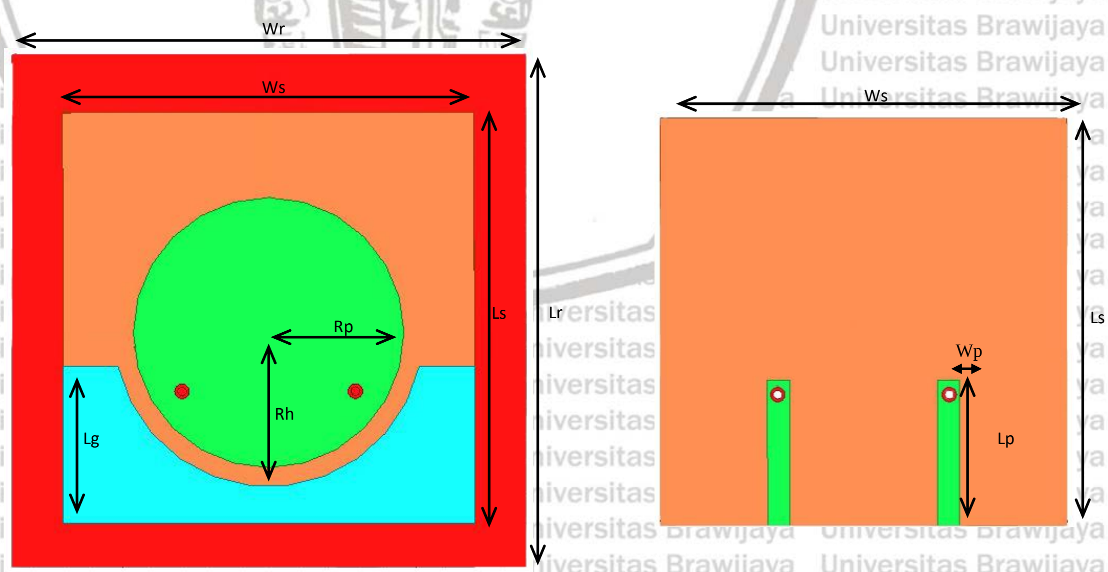


Figure 3-7 Dimensions of the microstrip antenna

Table 3-1. Dimensions of the microstrip antenna

| Variable | Dimensions (mm) |
|---|---|
| Wr | 35 |
| Lr | 35 |
| Ws | 30 |
| Ls | 30 |
| Rp | 9.2 |
| Rh | 10.5 |
| Lg | 10.7 |
| Wp | 1.5 |
| Lp | 10 |

The optimization process also determined the best distance between the antenna and the reflector as 7.5 mm. Notably, the via hole has a diameter of 6 mm and it is made of copper.

### 3.5.2 Branch-Line Coupler

After obtaining the dimensions of the branch-line coupler based on the theory, a simulation process was performed to obtain the S parameters of the branch-line coupler. The simulation was done using ADS, as shown in Figure 3-8. In this simulation, the optimization was used to change the dimensions of the branch-line coupler a little bit and also adjust the position of the antenna ports to see if the S-parameter results vary more closely to the ideal ones. As a result, the dimensions of the branch-line coupler after optimization are shown in Table 3-2 by referring to Figure 3-9. It is noted that the branch-line coupler uses the same substrate material as that of the microstrip antenna. Moreover, the shape of directional coupler was considered using HFSS to maintain the polarization of the antenna. It was found that the directional coupler affects the polarization and radiation patterns of the antenna if it has a wide shape.

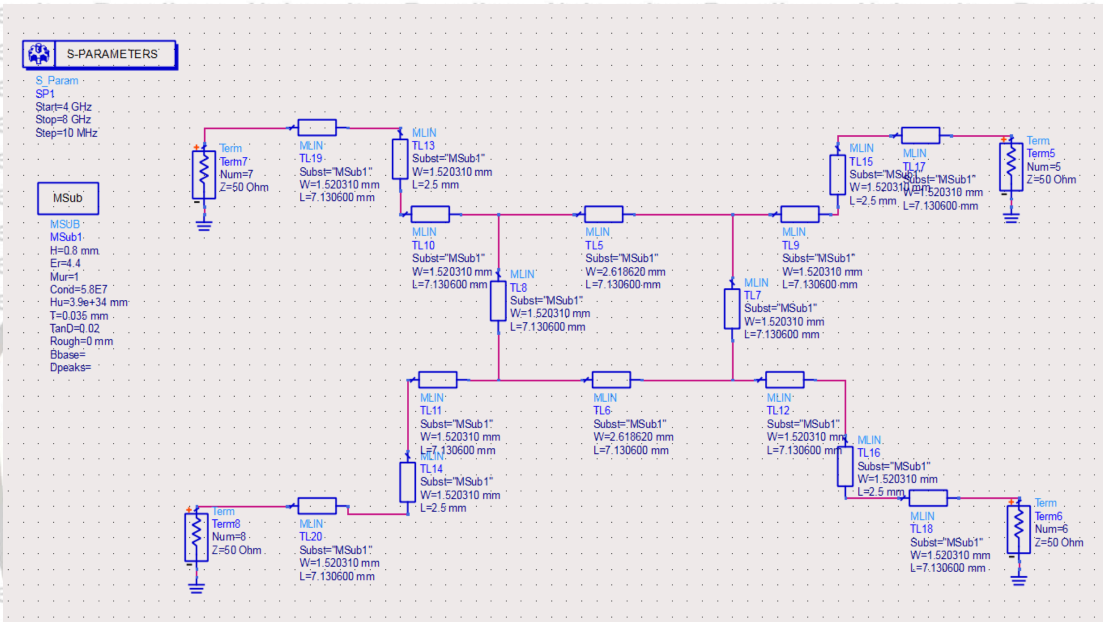


Figure 3-8 Branch-line coupler schematic in ADS

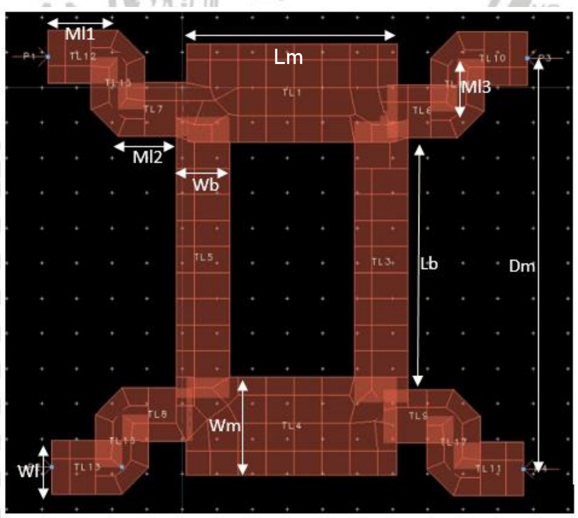


Figure 3-9 Dimensions of branch-line coupler

Table 3-2. Dimensions of branch-line coupler

| Variable | Dimensions (mm) |
|---|---|
| Lm | 35 |
| Wm | 35 |
| Lb | 30 |
| Wb | 1.5 |
| Wl | 9.2 |
| Ml1 | 10.5 |
| Ml2 | 10.7 |
| Ml3 | 5 |
| Dm | 1.5 |

## 3.6 Results and Discussion

This section includes the results and discussion of microstrip antenna, branch-line coupler, and the combination of both components.

### 3.6.1 Microstrip Antenna

The microstrip antenna was implemented according to its optimized dimensions in the simulation process, as shown in Figure 3-10. Then the antenna was measured to verify the antenna parameters such as bandwidth, gain, polarization, and radiation patterns. In the implementation, the microstrip antenna was connected with 50-Ohm SMA connectors for measurement purpose. Moreover, there is a plastic support between the reflector and antenna with negligible effect on the measurement results. Finally, the measurement results were compared with the simulation results, as shown in Figures 3-11 and 3-12, and the antenna performance was discussed accordingly.

(a)

(b)

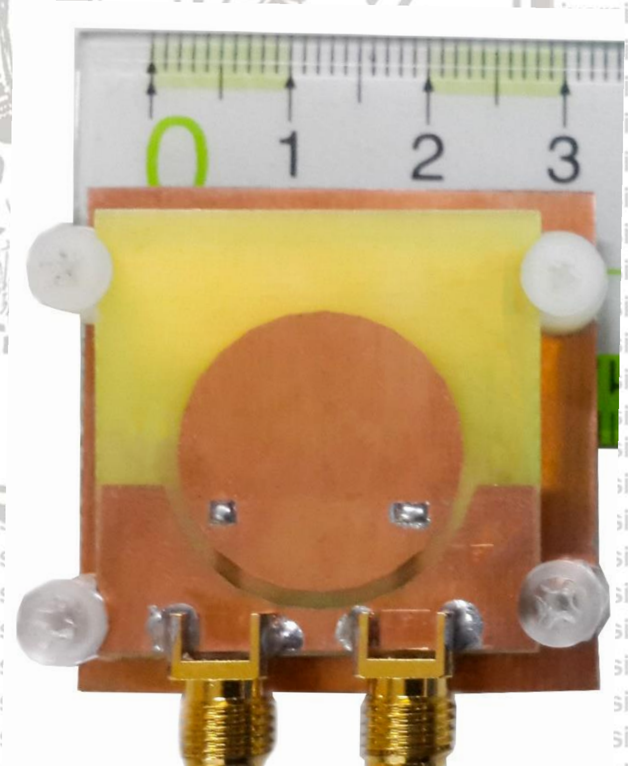


(c)

Figure 3-10 (a) Top view of the microstrip antenna. (b) Bottom view of the microstrip antenna (c) Top view of the microstrip antenna with the reflector

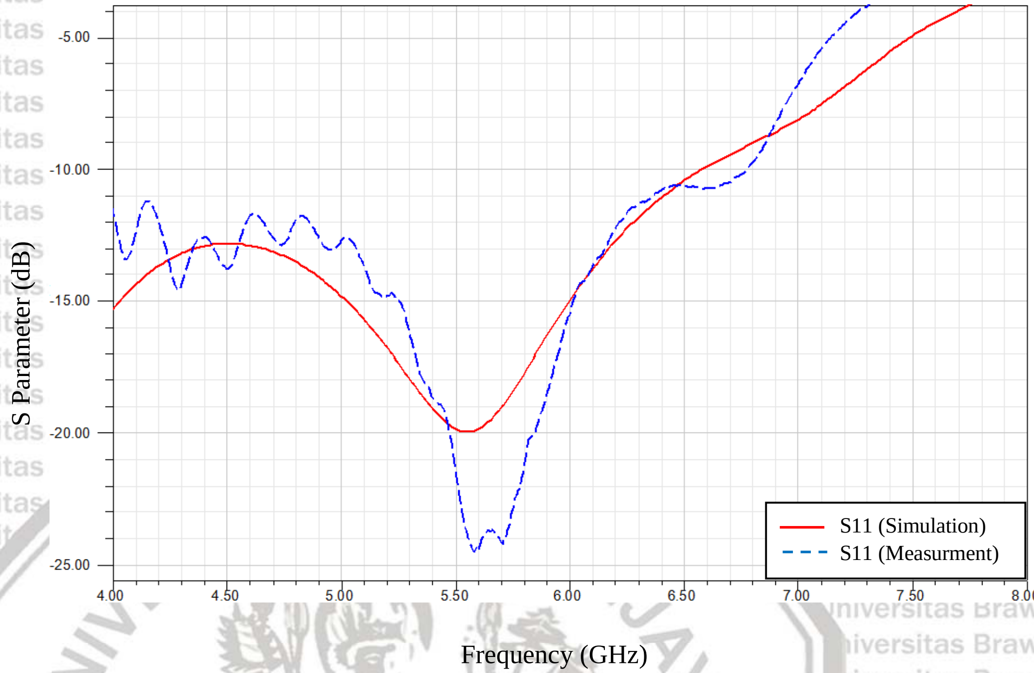


Figure 3-11 Magnitude of S11 of the microstrip antenna

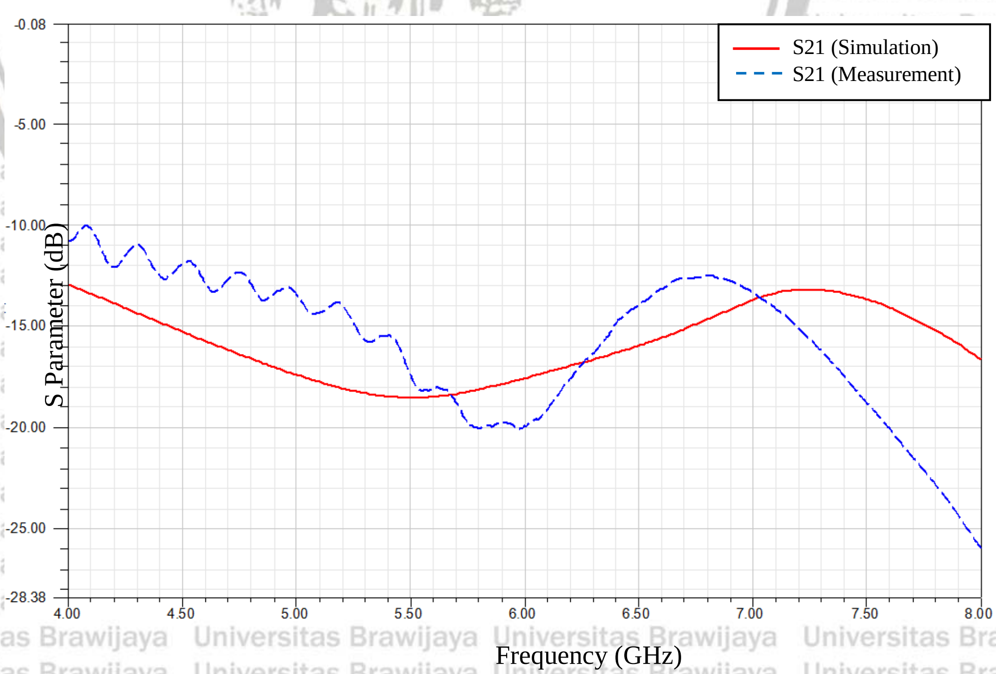


Figure 3-12 Magnitude of S21 of the microstrip antenna

Return loss is closely related to VSWR where the minimum return loss is 10 dB, corresponding to a maximum VSWR of 2 for meeting the specification requirement. The relation between the minimum return loss and maximum VSWR is shown as follows [13].

$$-10 \geq 20\log\ |\Gamma| \qquad \text{(Eqn.3-18)}$$

$$\geq\ |\Gamma|\ \leq \frac{1}{3}$$

$$\text{VSWR} = \frac{1+|\Gamma|}{1-|\Gamma|} \leq 2 \qquad \text{(Eqn.3-19)}$$

Tables 3-3 and 3-4 compare the return loss and VSWR of the microstrip antenna operating at 5.5 and 5.8 GHz, respectively. The measured results of return loss and VSWR meet the expected specifications. The comparison between simulation and measurement shows good agreement.

- Table 3-3 Port 1 or S11

| Frequency (GHz) | Simulation | | | Measurement | | |
|---|---|---|---|---|---|---|
| | S-parameter (dB) | Reflection Coefficient | VSWR | S-parameter (dB) | Reflection Coefficient | VSWR |
| 5.5 | -19.84 | 0.10 | 1.2268 | -21.22 | 0.09 | 1.1902 |
| 5.8 | -17.70 | 0.13 | 1.2995 | -21.31 | 0.09 | 1.1902 |

- Table 3-4 Port 2 or S21

| Frequency (GHz) | Simulation | | | Measurement | | |
|---|---|---|---|---|---|---|
| | S-parameter (dB) | Reflection Coefficient | VSWR | S-parameter (dB) | Reflection Coefficient | VSWR |
| 5.5 | -18.51 | 0.12 | 1.2693 | -17.39 | 0.13 | 1.3120 |
| 5.8 | -18.10 | 0.12 | 1.2841 | -20.00 | 0.10 | 1.2222 |

To determine the power transfer from or to an antenna, it is necessary to show the value of antenna terminal impedance. Figure 3-14 and 3-15 shows the impedance value based on the normalized value on the Smith chart. The normalized value on the Smith chart can also be seen as the impedance with the notation Rz in table 3-5 and 3-6.

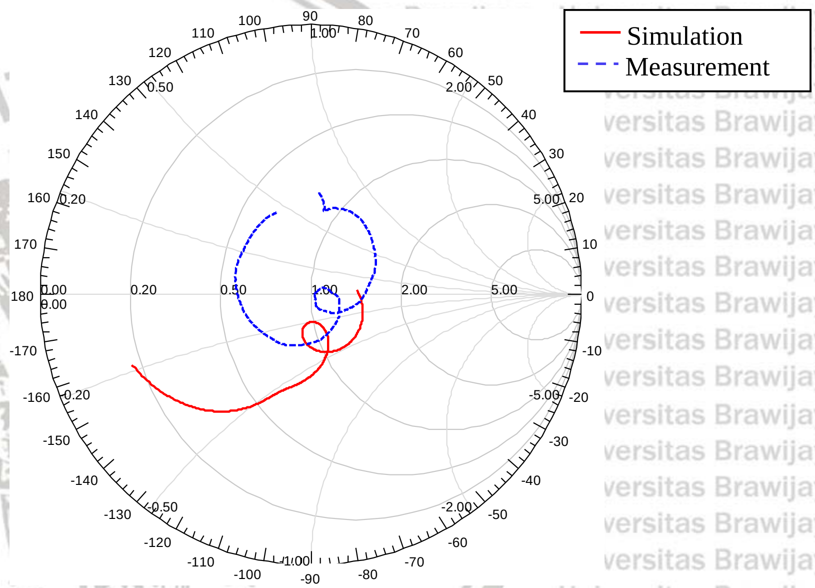


Figure 3-13 Smith chart impedance terminal Port 1 of the microstrip antenna

Table 3-5 impedance terminal Port 1

| **Frequency (GHz)** | **Simulation** | | **Measurement** | |
|---|---|---|---|---|
| | **Rx** | **Rz** | **Rx** | **Rz** |
| 5.5 | 0.97 - 0.19i | 48.57 - 9.49j | 1.05 - 0.11i | 52.32- 5.27j |
| 5.8 | 1.06 - 0.26i | 53.17 - 13.17j | 1.03 – 0.01i | 51.62 - 0.21j |

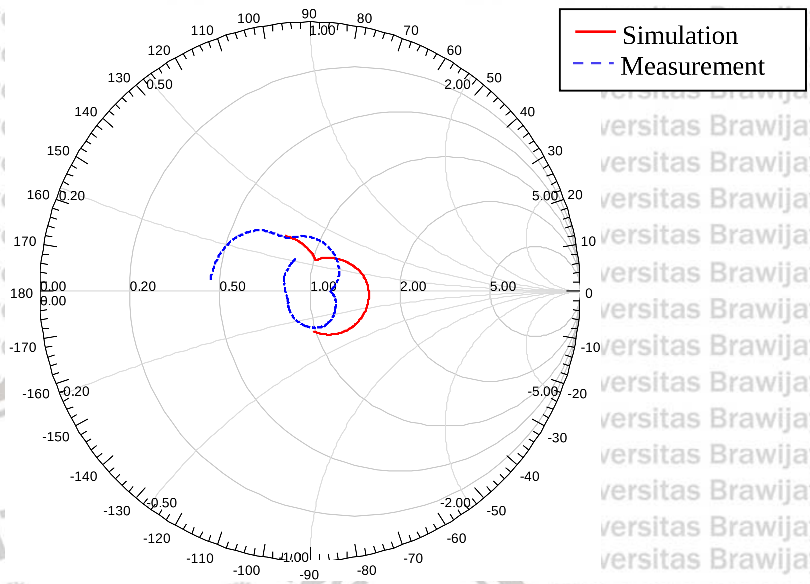


Figure 3-14 Smith chart impedance terminal Port 2 of the microstrip antenna

Table 3-6 impedance terminal Port 2

| Frequency (GHz) | Simulation | | Measurement | |
|---|---|---|---|---|
| | Rx | Rz | Rx | Rz |
| 5.5 | 1.02 + 0.24i | 50.88- 12.03j | 1.17 + 0.01i | 58.34 - 0.39j |
| 5.8 | 1.04 + 0.25i | 51.80- 12.63j | 1.19 + 0.02i | 59.29- 1.17j |

Table 3-5 and 3-6 shows the values of the Smith chart and inverse normalization so that the impedance value of each terminal for both simulation and measurement is known. The overall impedance value is close to 50 ohm. Thus the value is an appropriate value of the antenna requirement. So over all of the terminal impedance is a good agreement.

### 3.6.2 Branch-line Coupler

Figure 3-15 shows the implemented branch-line coupler with all four ports connected with 50 ohm SMA connectors for S-parameter measurement purpose. The simulated and measured S-parameter magnitudes are shown in Figure 3-16 and 3-17, respectively. The comparison between simulation and measurement shows good agreement.

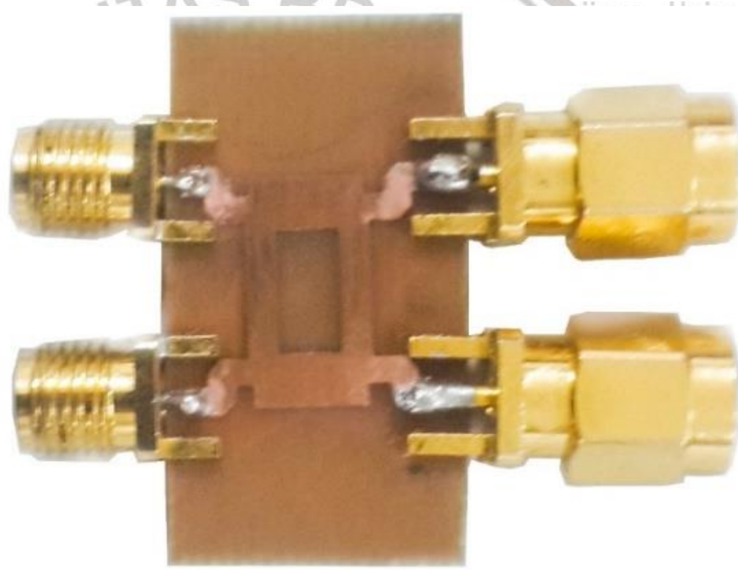

Figure 3-15 Implemented branch-line coupler

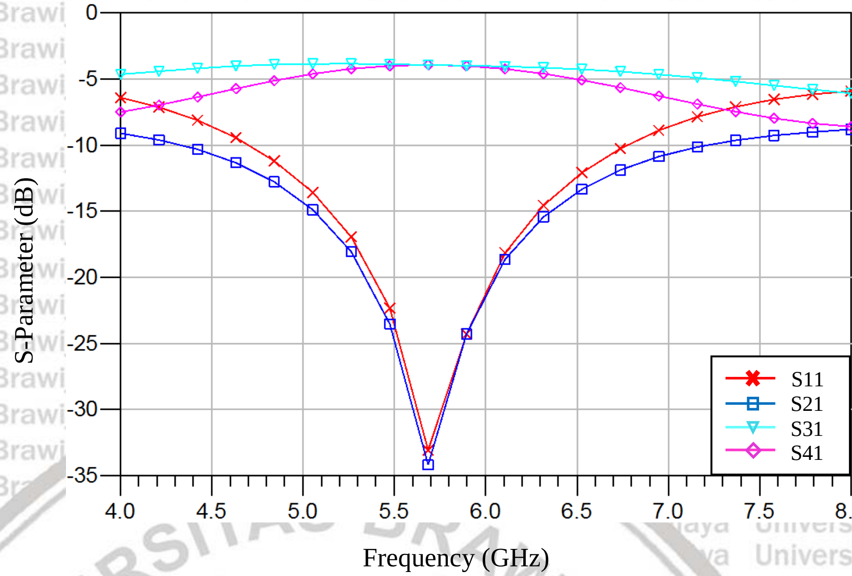


Figure 3-16 Simulated S-parameter magnitudes of the branch-line coupler

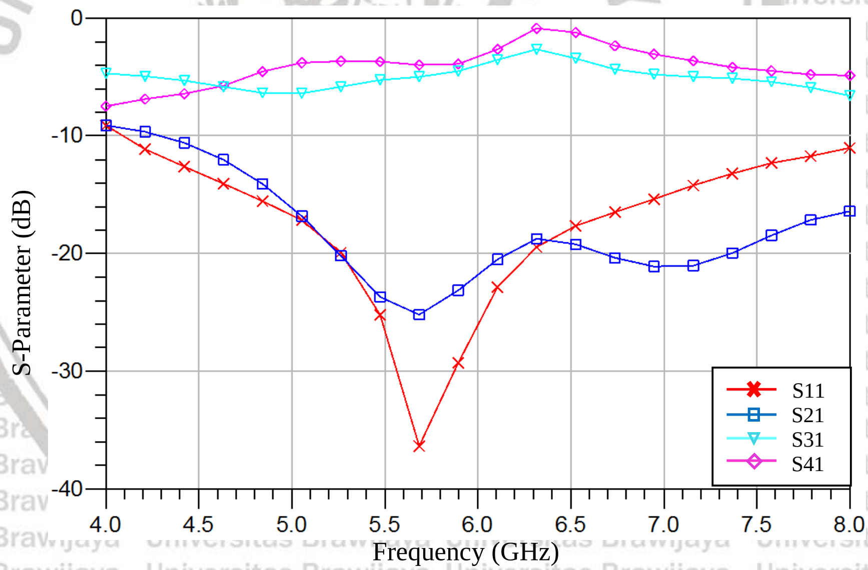


Figure 3-17 Measured S-parameter magnitudes of the branch-line coupler

Tables 3-7 compares the magnitude of S parameters of the branch-line coupler operating at 5.5 and 5.8 GHz, respectively. It can be seen from Table 3-5 that the measured magnitude difference between the two output ports is 1.5 and 0.71 dB at 5.5 and 5.8 GHz, respectively. Figure 3-18 and Figure 3-19 show the simulated and measured phases, respectively, of S31 and S41 of the branch-line coupler. Again, the comparison between Figure 3-18 and Figure 3-19 shows good agreement.

Table 3-8 summarizes the simulated and measured phases of S21 and S31 at 5.5 and 5.8 GHz. From Table 3-8, the phase difference between the two output ports of the branch-line coupler can be obtained, as shown in Table 3.7. It can be seen from Table 3-7 that the deviation of the measured phase difference from the ideal 90 degrees is less than 5 degrees in the frequency range from 5.5 and 5.8 GHz, which meets the expected specification.

Table 3-7 Comparison of S-parameter magnitudes of the branch-line coupler at 5.5 and 5.8 GHz

| S-Parameter | Simulation | | Measurement | |
|---|---|---|---|---|
| | 5.5 GHz | 5.8 GHz | 5.5 GHz | 5.8 GHz |
| S11 | -23.28 | -29.11 | -26.04 | -33.66 |
| S21 | -24.54 | -28.74 | -24.03 | -24.40 |
| S31 | -4.01 | -3.97 | -5.22 | -4.76 |
| S41 | -3.90 | -3.98 | -3.71 | -4.05 |

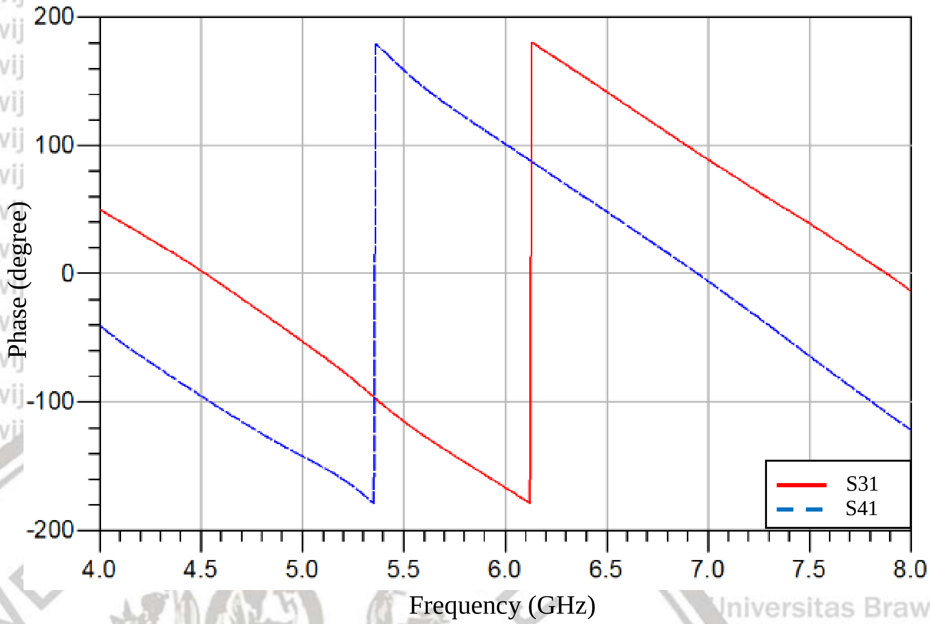


Figure 3-18 Simulated phases of S31 and S41 of the branch-line coupler

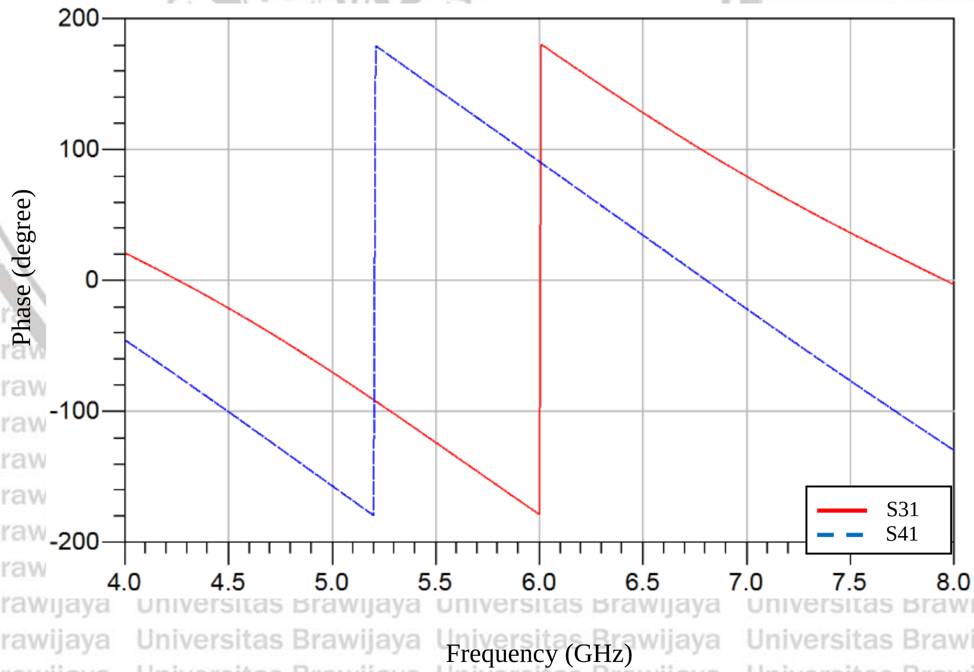


Figure 3-19 Measured phases of S31 and S41 of the branch-line coupler

Table 3-8 Comparison of the phases of S31 and S41 of the branch-line coupler at 5.5 and 5.8 GHz

| Phase | Simulation | | Measurement | |
|---|---|---|---|---|
| | 5.5 GHz (degree) | 5.8 GHz (degree) | 5.5 GHz (degree) | 5.8 GHz (degree) |
| S31 | -123.99 | -157.04 | -115.81 | -141.31 |
| S41 | 146.47 | 112.91 | 157.88 | 121.72 |

Table 3-9 Comparison of the output phase difference of the branch-line coupler at 5.5 and 5.8 GHz

| | Simulation | | Measurement | |
|---|---|---|---|---|
| | 5.5 GHz (degree) | 5.8 GHz (degree) | 5.5 GHz (degree) | 5.8 GHz (degree) |
| Phase difference | 89.54 | 90.05 | 86.38 | 90.98 |

### 3.6.3 Connected Microstrip Antenna and Branch-line Coupler

The microstrip antenna and branch-line coupler are connected using the SMA connectors, as shown in Figure 3-20. Once connected, to know whether the antenna and branch-line coupler function or not, the S11 and S21 parameters i.e. the reflection and isolation, were measured, as shown in Figure 3-21. It can be seen from Figure 3-21 that the magnitudes of S11 and S21 are -20.17 and -22.13 dB, respectively, at 5.5 GHz, and -14.97 and -14.57 dB, respectively, at 5.8 GHz. Both parameters are less than -10 dB over the frequency range of interest, showing that the connected microstrip antenna and branch-line coupler function properly. In addition to these two S parameters, the antenna parameters such as radiation pattern, polarization, efficiency and gain were also measured.

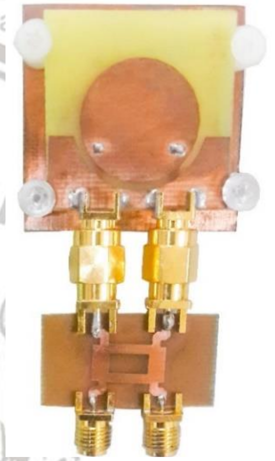

Figure 3-20 Connected microstrip antenna and branch-line coupler

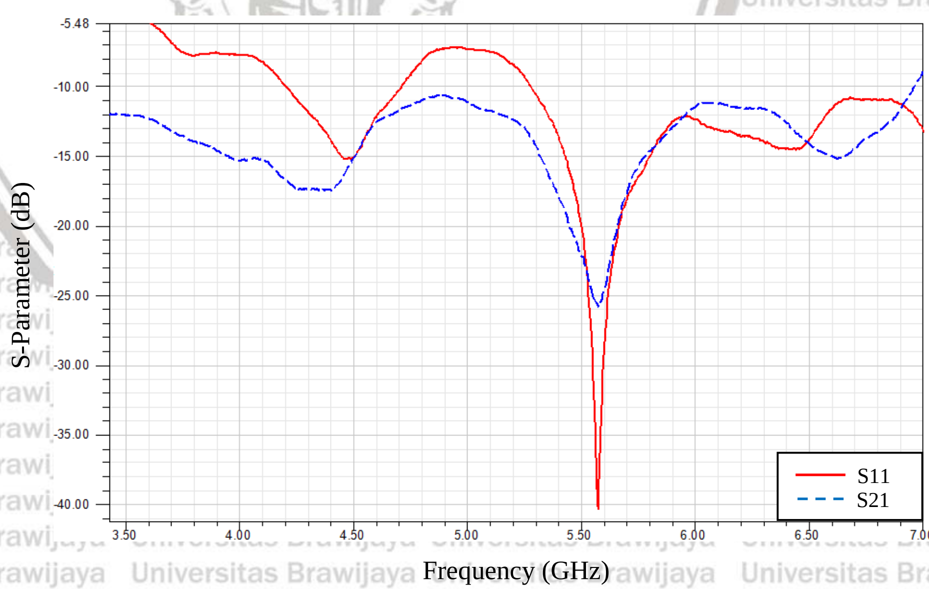


Figure 3-21 Measured S-parameter magnitudes of the connected microstrip antenna and branch-line coupler

Generally speaking, the conventional microstrip antennas have a low gain. Therefore, the microstrip antenna presented in this thesis uses a reflector to increase its gain, as shown in Figure 3-12. As a result, Figure 3-22 compares the simulated and measured gain of the presented microstrip antenna. It can be seen from Figure 3-22 that the measured gain of the antenna ranges from 3.7 to 5.5 dBi over 5.5-5.8 GHz.

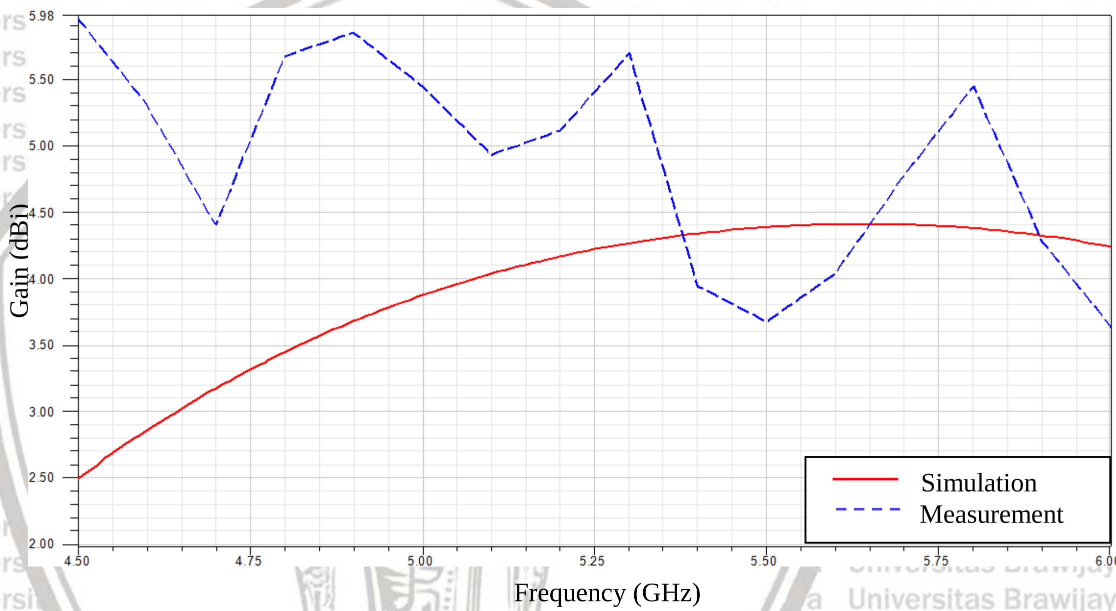


Figure 3-22 Comparison of the simulated and measured gain of the microstrip antenna

The efficiency of the microstrip antenna can be further calculated by [1]

$$\eta = \frac{10^{\frac{G}{10}}}{\left(\frac{\pi D}{\lambda}\right)^2} \qquad \text{(Eqn.3-20)}$$

where G is the gain; D is the diameter or maximum width of the reflector, and λ is the wavelength. Figure 3-23 compares the simulated and measured efficiency of the microstrip antenna. It can be seen from Figure 3-23 that the efficiency of the microstrip antenna ranges from 52% to 78% over 5.5-5.8 GHz.

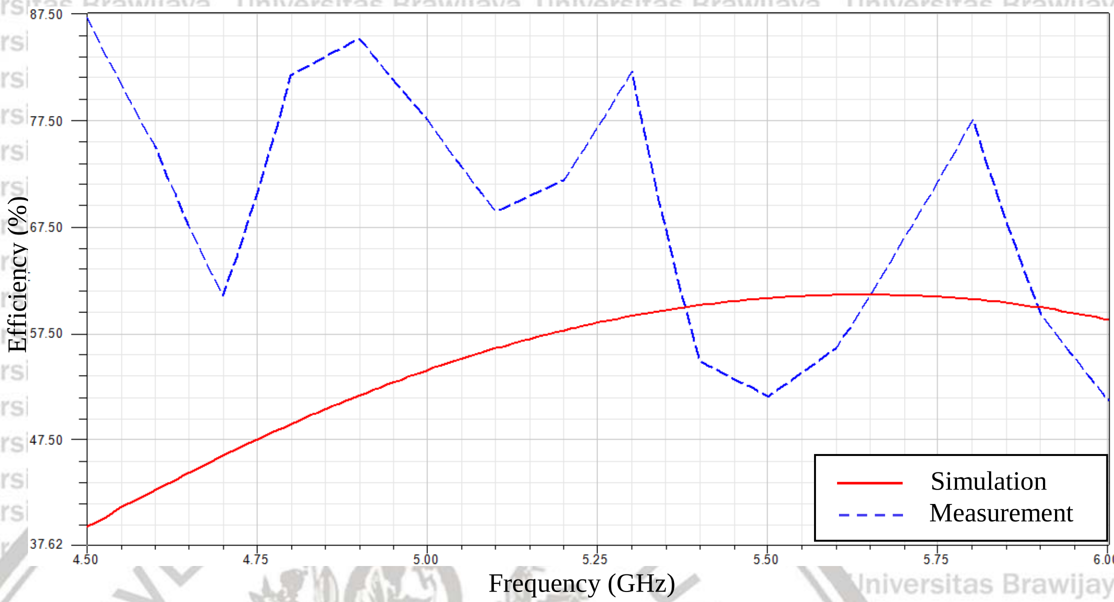


Figure 3-23 Comparison of the simulated and measured efficiency of the microstrip antenna

Figure 3-24 shows the axial ratio of the microstrip antenna when excited with circular polarization. It can be seen from Figure 3-24 that the measured axial ratio is 10.68 and 7.82 dB at 5.5 and 5.8 GHz, respectively. Therefore, the microstrip antenna is considered to have a linear polarization. The disagreement between simulation and measurement results from the non-ideal interconnection between the branch-line coupler and the microstrip antenna. The resulting effect causes the two excited waves that are transmitted from the microstrip antenna to be not linearly perpendicular to each other. Moreover, these two excited waves have a considerable magnitude difference from one to the other, which is also responsible for the circular polarization degradation. The improvement of the circular polarization can be made by designing the microstrip antenna and branch-line coupler together on one board to reduce the size of ground plane of the microstrip antenna and the branch-line coupler.

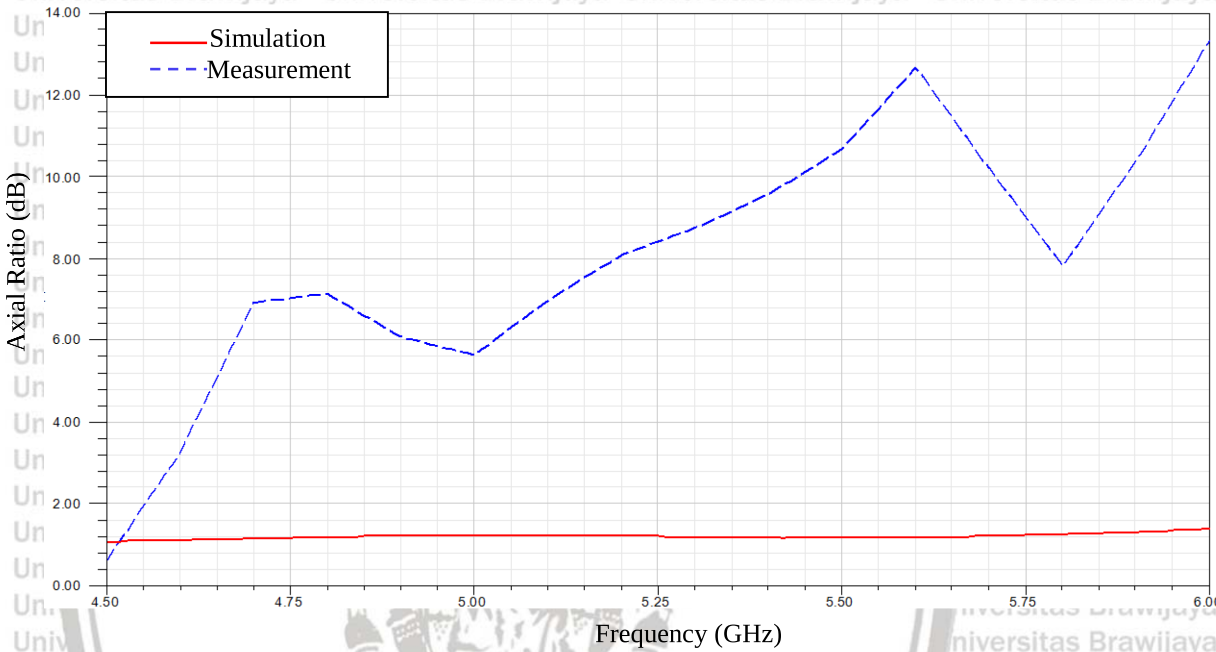


Figure 3-24 Comparison of the simulated and measured axial ratio of the microstrip antenna

Although the radiation patterns are frequency dependent, they are basically similar over a narrow frequency range. Therefore, the measured and simulated radiation patterns were taken only at 5.5, 5.6, 5.7 and 5.8 GHz in this study. Radiation patterns are three-dimensional and can be viewed in terms of the two-dimensional H-plane and E-plane patterns that vary with respect to the angle phi and the angle theta, respectively.

Figure 3-25 and Figure 3-26 show the measured and simulated H-plane patterns and E-plane patterns, respectively, at 5.5, 5.6, 5.7 and 5.8 GHz. The comparisons between simulation and measurement show good agreement. It can be seen from Figure

3-25 and Figure 3-26 that the radiation patterns can be regarded as directional because their main lobes are much stronger than their back lobes.

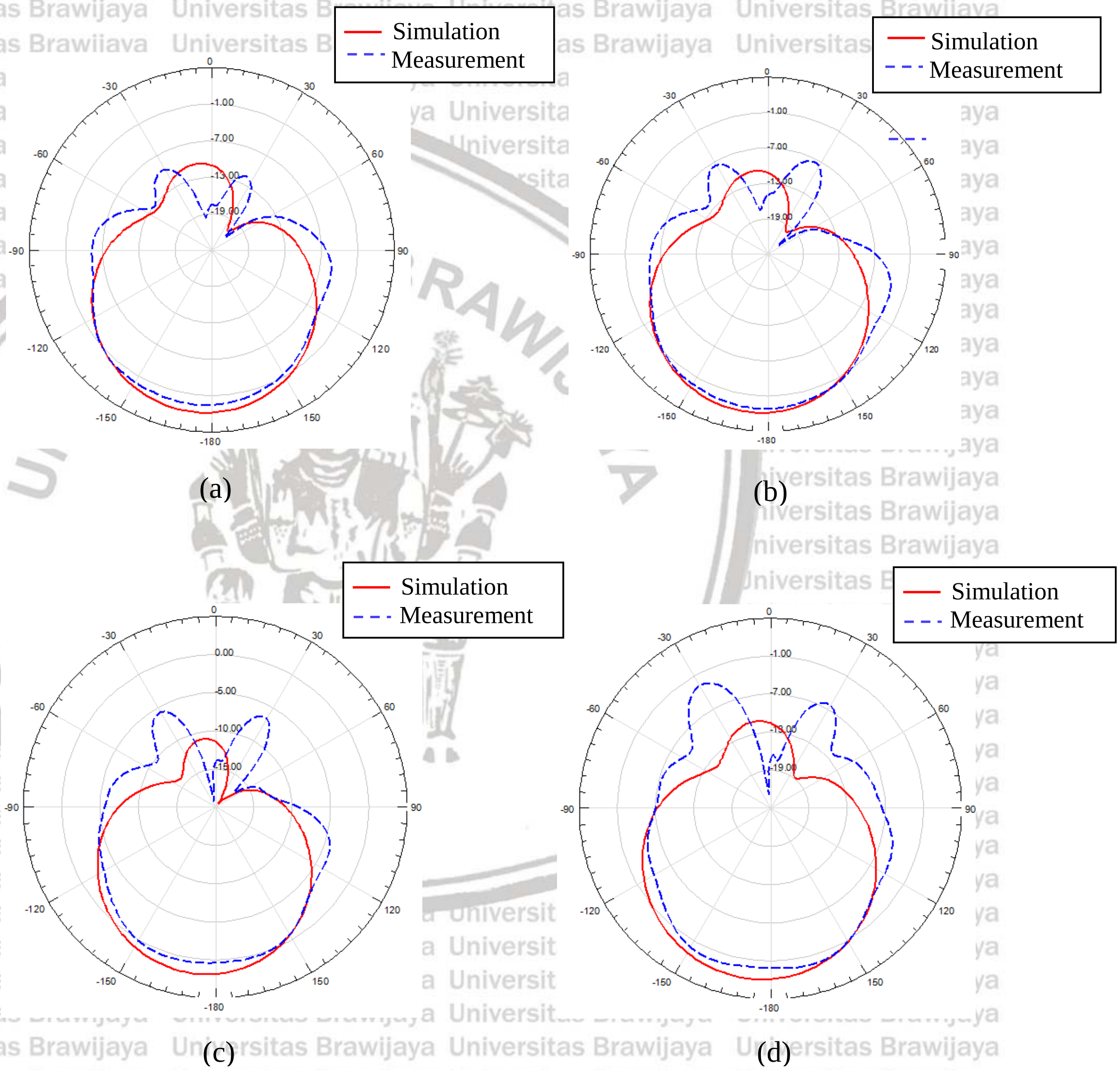


Figure 3-25 Simulated and measured H-plane radiation patterns of the microstrip antenna (a) 5.5 GHz (b) 5.6 GHz (c) 5.7GHz (d) 5.8GHz

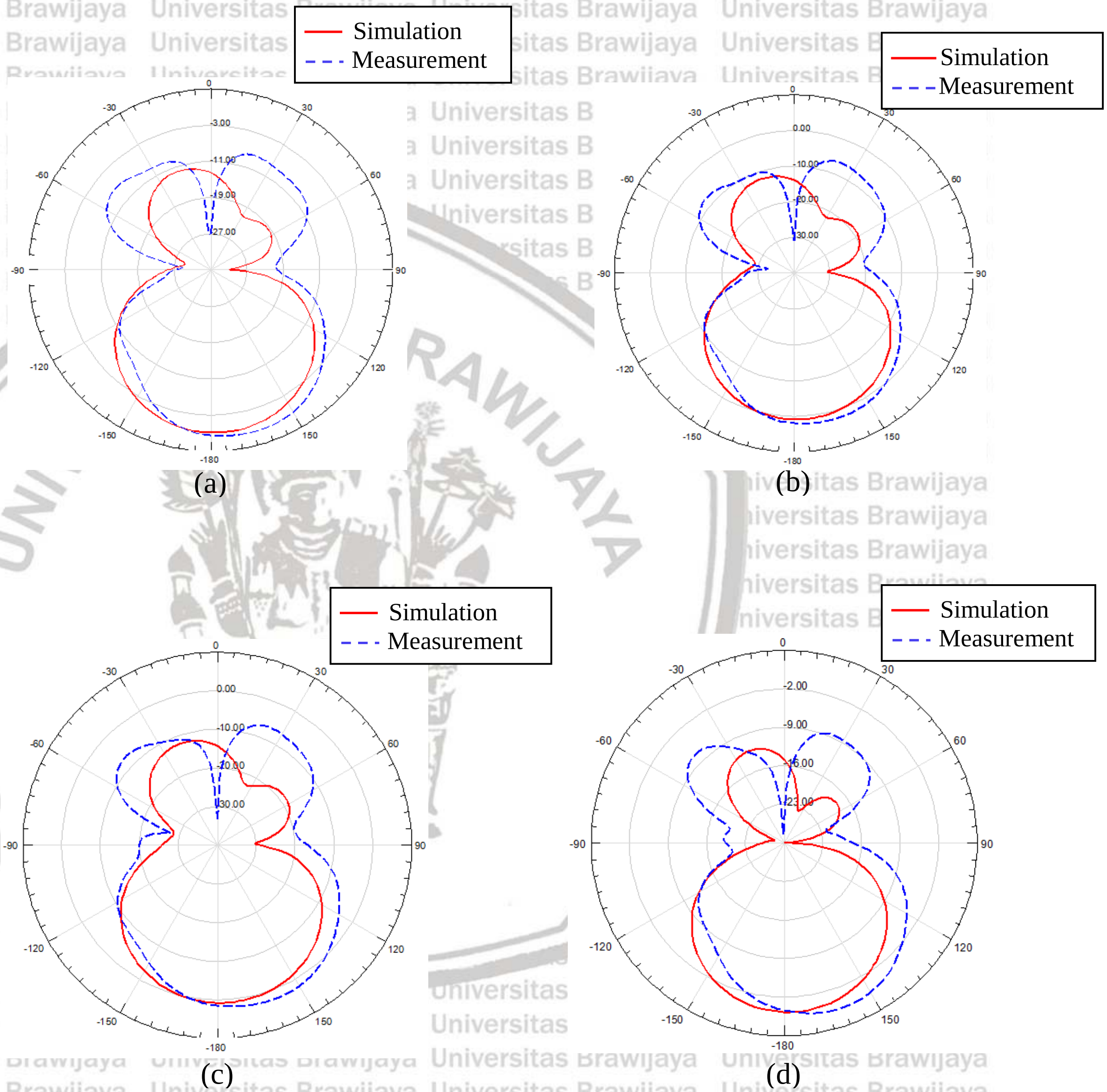


Figure 3-26 Simulated and measured E-plane radiation patterns of

the microstrip antenna P(a) 5.5 GHz (b) 5.6 GHz (c) 5.7 GHz (d) 5.8 GHz

# Chapter 4. CONCLUSION

In this thesis, a microstrip antenna with a connected branch-line coupler with an overall dimension of 35 mm × 70 mm was presented. The antenna has an operating frequency range from 5.5 to 5.8 GHz, and an output phase difference of 86.384 and 90.978 degrees at 5.5 and 5.8 GHz, respectively. Moreover, the antenna has a directional radiation pattern and a linear polarization. Its gain and efficiency are 3.67 dBi and 52% at 5.5 GHz, and 5.45 dBi and 78% at 5.8 GHz.

# References

[1] Balanis, C.A, Antena Theory: Analysis and Design, 3rd Edition. John Wiley and Sons, Inc. 2005, pp. 27, 80, 72, 30,66-68, 20-21.

[2] Balanis, C.A, Antena Theory: Analysis and Design, 4rd Edition. John Wiley and Sons, Inc. 2016, pp. 5

[3] David M. Pozar, Microwave Engineering, 3rd ed., John Wiley and Sons, Inc. 2005, pp. 317.

[4] E.R. Escobar, N.J. Kirsch, G. Kontopidis and B. Turner, "5.5 GHz optically transparent mesh wire microstrip patch antenna", *IEEE Electronics Letters*, Vol.51: 1220, 2015.

[5] Yu-Hsuan Lin and Huei Wang, "A Low Phase and Gain Error Passive Phase Shifter in 90 nm CMOS for 60 GHz Phase Array System Application", *IEEE Electronics Letters*, 978-1-5090-0698-4/16, 2016.

[6] Yasushi Itoh, Hiroaki Takagi, "A Dual-Band 90-Degree SiGe HBT Active Phase Shifter Using Band-Pass and Band-Stopsigns", *IEEE Proceedings of the 47th European Microwave Conference,* Nuremberg, Germany, pp. 232, 2016.

[7] Donald K. Weaver, Design Of Rc Wide-Band 90-Degree Phase-Difference Network*", IEEE Proceedings Of The I-R-E.* Caliif, pp: 671, 2016

[8] Chung-Yi Hsu, Cho-Ying Chuang, Fu-Kang Wang, Tzyy-Sheng Horng, and Lih-Tyng Hwang, "Detection of Vital Signs for Multiple Subjects by Using Self-InjectionLocked Radar and Mutually Injection-Locked Beam Scanning Array", *IEEE Proceedings*. Kaohsiung 804, Taiwan, Vol : 978-1-5090-6360-4, 2017.

[9] Abdolmehdi Dadgarpour, Ahmed A. Kishk, Tayeb A. Denidni, "Dual band high-gain antenna with beam switching capability", *IET Microwave Antennas Propagation*,Vol. 11 Iss. 15, pp. 2155-2161, 2017.

[10] Peng Gao, Shuang He, Xubo Wei, Ziqiang Xu, Ning Wang, and Yi Zheng, "Compact Printed UWB Diversity Slot Antenna With 5.5-GHz Band-Notched Characteristics", *IEEE Antennas And Wireless Propagation Letters*, Vol. 13 : 1536-1225, 2014.

[11] A. Abdel-Rahman, A. R. Ali, S. Amari, and A. S. Omar, "Compact bandpass filters using defected ground structure (DGS) coupled resonators," in IEEE MTT-S Int. Microw. Symp. Dig., 2005, pp. 12–17.

[12] David M. Pozar, Microwave Engineering, 3rd ed., John Wiley and Sons, Inc. 2005, pp. 49-156.

[13] Nakar, Punit S¸ "Design of a Compact Microstrip Patch Antena for use in Nirkabel/Cellular Devices", *Thesis. The Florida State University*, pp : 19,40, 2004.

[14] Edgar Hund, "Microwave Communications: Components and Circuits", *ISE Editions, McGraw-Hill Education,* pp : 43, 1989.

[15] Liao, S, "circuit and analysis amplifier design, Prentice-Hall International", Englewood Clifs NJ, pp : 140, 1987

[16] Peter. W. Gorham, "Power Dividers And Directional Couplers", *University of*

*Hawai'i at Manoa handbook,* Jeff Kowalski, pp. 6-41.

[17] Marc E. Goldfarb and Robert A. Pucel, "Modeling Via Hole Grounds in Microstrip", *IEEE Microwave and Gided Wave Letters,* Vol. 1 No. 6, June 1991

[18] J. Yamasaki, I. Ohta, T. Kawai, and Y. Kokubo, "Design of broadband semi-lumped and lumped-element quadrature hybrids" ,*IEEE Microwave Theory and Techniques Society International Microwave Symposium,* Long Beach, California, USA, DOI: 10.1109/ MWSYM, 2005.

[19] T. Hirota, A. Minakawa, and M. Muraguchi, "Reduced-Size Branch-Line and Rat-Race Hybrid for Uniplanar MMIC's," *IEEE Trans. Microwave Theory Tech.,* vol. MTT-38, pp. 270-275, March 1990.

[20] Jun Wu and Lu-Yu Wang, "Analysis and Design of a 3 dB Tunable Lumped-Element Directional Coupler", *Journal Of Electronic Science And Technology,* Vol. 8, No. 2, June 2010.